General Comments

First of all we would like to thank the reviewers for their thorough read through the manuscript and their constructive comments. We have completed the revision of the manuscript exactly as listed in the response to the interactive comments and for reference these responses are inserted below.

Additionally, we have added a reference to the paper by Paul et al (2019), where the co-author Matthias Haeckel has recently published a selection of geochemical data that are also presented in this paper. Some references were updated to their current state of publication.

One of the authors names were changed to its use in scientific publication (Janssen instead of Janßen).

We have also adjusted the acknowledgements to include the grant number not only of the first but also of the current second phase of the MiningImpact project.

Attached is a tracked version of the revised manuscript (as pdf). It was not possible to track changes made to endnote-controlled references so we have highlighted them individually in yellow.

Response to interactive comment on "DISCOL experiment revisited: Assessing the temporal scale of deep-sea mining impacts on sediment biogeochemistry" by Laura Haffert et al.

Anonymous Referee #1

This paper covers an important subject, which should be of interest to the readers of Biogeosciences. The major finding of this study is the differences in recovery time of deep sea sediments between two methods that can be used during deep sea mining. The authors used an extensive dataset and model porewater and solid phase depth profiles with numerical a numerical model.

In general I think the structure of the paper is a bit confusing. There is an introduction section (section 1) but within this section there is a long discussion/introduction of the general biogeochemistry of the Peru Basin (section 1.1). I think this would be more in place in the methods section as a site description.

The results section contains a lot of discussion where I think it should be better to first clearly describe all the data, which is used in this study. The discussion section is rather short and reads as a conclusion part. I think the discussion and conclusion part can be combined. I think the manuscript is highly under referenced.

As described in more detail in later responses to comments directly related to each section, we will restructure the document and suitable references will be added.

Abstract:

Line 19: "reduces seafloor nutrient fluxes over centuries" - I think based on this study the authors can only draw conclusions for oxygen. Otherwise the authors should include more data from their modelling study on the effects of these two different sampling techniques. Now the only information given in the discussion (and figures 10 and 11) are oxygen fluxes. I think it would be a good addition to also show other nutrients fluxes from the sediment (for example ammonium/nitrate), which are already in the model I guess.

Figure 10 and 11 focus on oxygen profiles because of the central role that the oxygen penetration depth plays. Figure 12 depicts seafloor fluxes of nutrients and here we will add the seafloor fluxes of NH4 and NO3 over time to the flux diagram 12B.

Can the authors also give some information about the changes/recovery of macrofaunal communities.

We will add a sentence at the end of the abstract addressing faunal recovery: 'The interdisciplinary (geochemical, numerical and biological) approach highlights the closely linked nature of benthic ecosystem functions, e.g. through bioturbation, microbial biomass and nutrient fluxes, which is also of great importance for the system recovery. ***It is, however, important to note that the nodule ecosystem may never recover to pre-impact state without the essential hard substrate and will instead be dominated by different faunal communities, functions and services'****.*

More specific analyses of changes / recovery of macrofauna is beyond the scope of this study.

Introduction:

In my opinion section 1.1 is a bit out of place. This section describes processes that are important in general (degradation of organic matter P2 lines 55-59). I would move this to the introduction and make a new section 2.1 with a site description where you discuss all the processes that are important for your study. Also I think this part is under referenced.

We will move this section to the methodology section and rename it to 'Biogeochemical site description'. Only very few studies give detailed information on the biogeochemistry of the area. The repetitive use of these reference throughout the text is impracticable so that the main references are introduced before the specific site description: 'König et al. (1999), König et al. (2001) and Haeckel et al. (2001) have previously identified and quantified through diagenetic modelling the main biogeochemical processes in the Peru Basin, including the DEA region.' We will add a colon after this sentence to emphasize that the following information belongs to these references.

In lines 39-41 you describe there were studies that focused on characterization and distribution of macrofauna. I think it would good to shortly explain what was found in these studies in this section because disturbance of macrofauna is important as you also describe in you abstract.

We will add references to the sentence (Line 41):

*The DISCOL experimental area (DEA) was revisited before and several times after the initial disturbance, with research concentrating mainly on the characterization and distribution of benthic fauna (**e.g. Borowski and Thiel, 1998; Borowski, 2001; Bluhm, 2001**).*

And we will add here a sentence on macrofaunal abundances:

'Macrofaunal communities, which are particularly important for the bioturbation and thus redox zoning of the sediment, are mainly composed of Polychaeta (about 50%) and to a lesser extent tanaidacea (10 - 20%) and bivalvia (5 – 10%) (Borowski and Thiel, 1998). After the artificial disturbance, very few faunal groups returned to baseline or control conditions after more than two decades (Jones et al., 2017) and the main mode of macrofaunal recolonization was found to be via lateral migration (Borowski and Thiel, 1998).'

I think the last paragraph of this section is a bit out of place or should be better introduced.

We will move this section, which intends to justify the introduction of a shallow Fe(II)-O2 reaction layer, to the description of the diagenetic model to Line 180:
'The reaction network shaping the geochemistry of the upper sediment metres, namely organic matter degradation and secondary redox reactions including the oxidation of ammonium and dissolved manganese, are listed in Table 3 as well as the corresponding rate expressions. We also included a shallow semi-labile Fe(II) layer that reacts with oxygen to the model (Figure 2). While it is established that a labile Fe(II) reaction front impedes the downward migration of nitrate (König et al., 1997;König et al., 1999), little is known about the redox potential of Fe(II) on different crystallographic lattice positions (coordination sites) in clay minerals, such as nontronite. In particular, information is lacking on the reactivity of the Fe(II) on these sites with respect to oxidation by nitrate and oxygen. Available Mößbauer data (König et al., 2001) from the DISCOL area indicate a refractory fraction of Fe(II) that prevails in the nitrate reduction zone (~10 % of total iron). In the light of the much higher redox potential of oxygen compared to nitrate, we model the remaining Fe(II) as a semi-labile phase representing a second reaction front impeding the downward migration of oxygen.'

Results:
It is quite difficult to understand to which plots you refer in this section. Add more figure numbers behind your statements.

We will add more Figure references to the statements.

Also the order of discussing data is a bit strange. You start with porosity but this is plotted in figure 5. You should start with describing figure 3 or change the order of figures.

We will reorder Figure 3-5, beginning with the solid composition of the sediment.

There is a lot of discussion in section 3.1. I think it would be better to first describe the porewater and solid phase profiles (in order of the figures) before you start your discussion.

In section 3.1 observed porewater trends are described in the context of well-established processes (e.g. nitrate decline through denitrification in anoxic sediments; relating manganese oxide reduction to the increase in dissolved manganese in anoxic sediments; linear profile shape indicates reaction front, etc). The structure of the results follows other examples in this field (e.g. Haeckel et al., 2001) and we believe that by providing a process-oriented description of the results, the discussion can better focus on the actual objectives of this manuscript.

Section 3.3 Most of the interesting statements in this section are based on Vonnahme et al submitted or at visual observations. There is not a good link with the data shown in figures 4-6. I think it would be better to compare these instead of discussing visual observations or "repeating" findings presented in Vonnahme et al. submitted.

We would like to disagree with the reviewer in this point. Section 3.3 is a chapter on impact characterization. It includes (i) a physical description of the disturbance, (ii) references to result figures, where relevant differences of the impacted to reference sites can be noticed (oxygen profiles, porosity profiles, dissolved manganese) and (iii) information on a parallel microbiological study (Vonnahme et al, submitted), which is by nature closely interlinked with the biogeochemical processes discussed in this manuscript. Information on microbiological activities (the Vonnahme et al. paper) are not 'repeated' in a separate paragraph but are instead added throughout the text supporting the characterization of different impact types.

Conclusions
I suggest to strongly shorten this section and only discuss the main conclusions found in this study and not discuss conclusions from other studies.

The conclusion paragraphs are structured as follows:

- *Highlighting the importance of the updated diagenetic transport-reaction model, especially with respect to the newly introduced Fe(II)-O2 reaction layer.*
- *Summarizing the outcome of the prognostic model by simply listing the three stages of recovery*
- *A holistic (interdisciplinary) summary of the mining impact, highlighting the close link between geochemical and biological processes*

These three paragraphs directly link to the three research aims in the introduction.

The last paragraph of the conclusion draws the larger picture of the impact of nodule mining in the deep-sea, which is not only applicable beyond the studied site but is also important for the non-expert readers who base regulatory decisions on publications like these.

The authors have carefully structured the conclusions, which are in line with the guidelines of the publishers. We would thus like to maintain the structures as it is.

Figures:
The resolution of the figures could be improved.
The resolution issue is an artefact of the pdf converter of the journal webpage. The original files have much higher resolution.

Detailed comments: Line 17: "(micro)-biological data". Is this in place? There is no microbiological data in this manuscript.

Microbiological abundances are stated throughout the text (for example in the 'impact characterisation') and are related to the availability of labile organic matter and consequences for the food web structure in the discussion. Figure 12 also plots some microbial abundances for comparison.

Line 18: how was the depth of this reactive surface layer quantified.

The reactive layer was determined, on one hand, simply by its distinct dark brown colour and, on the other hand, by the oxygen penetration depth. This is described in the section 'Geochemistry of the DEA region: 'The upper reactive sediment section (up to ~20 cm.b.s.f) is markedly different from the deeper sediment sections. It is characterized by a sharp decrease in porosity (from 0.94 to approx. 0.86, Table 4) and is rich in manganese oxides (Paul et al., under review), which gives this layer its distinct dark brown color.[…] In situ oxygen profiles confirm that the upper brown layer represents the oxygenated zone (Figure 6). In this zone, oxic respiration of organic matter not only consumes downward diffusing oxygen […]'.

Line 19: "reduces seafloor nutrient fluxes over centuries". From sediment towards the water column? Maybe say benthic release of nutrients.

We will change the sentence accordingly

Line 39: col in recolonization should be in capitals similar to dis in disturbance

Yes indeed, the 'col' should have been capitalized which will be amended.

Line 43: introduce abbreviation of ROV

We will change it to '[…] remotely operated vehicle (ROV) […]'

Line 47: What do the authors mean with a "state of the art geochemical dataset". I think it would be more appropriate to call the data set extensive, which is indeed the case when taking into account the amount of profiles.

For the research aim at hand, the authors intended to highlight that the dataset is not only extensive but includes state-of-the art data (like oxygen profiles from TV guided sampling stations, as described in the paragraph above), which were not available when the first diagenetic model was published in 2001 and thus justifies the presentation of this new modelling work. We will change to '[…] comprehensive set of data obtained with state-of-the-art methodology[…]'

However, I would suggest to also include porewater iron as this variable is discussed multiple times throughout the manuscript.

Porewater iron concentrations are all near or below detection limit and this is described in the text (Line 226).

Line 61-63: how deep is the layer where there is organic matter degradation? Does this mean there is no iron of sulfate reduction?

There is iron(III) reduction deeper in the sediment as witnessed by the tan-green color change in the sediment. The specialty in the Peru Basin is that the reduced Fe is not released into the porewater (thus dissolved Fe remains below or near the detection limit) but is incorporated into the clay mineral phase. SO_4 reduction is not reached however. See Haeckel et al., 2001.

Line 64: which depth is the bioturbation depth approximately?

One highlight of the paper is that the bioturbation depth is derived from radiometric data, which is presented in Figure 7 and discussed in the section 'Diagenetic reference model'. The bioturbation depth reaches at least 10 cm, at which point the bioturbation intensity rapidly declines until around 15 cm below the seafloor.

Line 65: "Oxygen is depleted at a sediment depth of 5 to 15 cm, " Do you mean in general for deep see sediments? Then add a reference.

No, this statement is located in the section 'Biogeochemistry of the Peru Basin' and is thus valid for the Peru Basin and taken from the references that are introduced three sentences before. As discussed for a comment further up, we will better clarify the sources of information for this section.

Line 65: "with the DEA region being on the deeper end". Add reference.

Please see comment above

Line 66: "In the slightly shallower region of the Peru Basin seawater-derived nitrate and nitrate from oxic respiration is consumed within the bioturbated upper 20 cm of sediment". Add reference.

Please see comment above

Line 70: It is a bit confusing to also refer to this layer as reaction layer as you also have a surface 'reaction layer'. I would use a different name iron-rich layer for example.

We will remove 'reaction' for the description of the Fe(II)-rich layer to avoid confusion with the surface 'reaction layer'.

Line 70: "formed during glacial times". Approximately how long ago?

We will add: ',(corresponding to an age of at least 60 ka)'

Line 70: add reference to :" This reaction layer was formed during glacial times, when organic matter deposition was strongly increased and potential electron acceptors such as oxygen, nitrate and manganese oxide were exhausted closely below the sediment surface. "

We will add the reference (König et al., 2001).

Line 79-85: Is this one of the main research questions? This is not described in the abstract.

No. It is simply a justification of our presented modelling approach. As described above, we will move this paragraph to the description of the diagenetic model.

Line 89: “to artificially disturb the”. This means without removing the reactive surface layer?

Exactly, during the DISCOL experiment the sediment was ploughed but not removed. However, as part of this follow-up survey, a fresh disturbance was created with an epibenthic sledge, which removed the upper sediment layer and piled it up at the side of the track. Because the difference between ‘ploughing’ and ‘removing’ is indeed important, we highlighted the difference in the section ‘Impact characterisation’.

Line 92: what does less disturbed mean. The sediment depth of disturbance?

The effects of disturbance are manifold and include sediment mixing, displacement and blanketing with resettling sediment. ‘Less disturbed’ would for example be the description of an area that was affected only by a thin layer of resettling sediment. The gradient of disturbance plays an important role for this paper and is described in more detail in the impact characterization.

Line 97: I would give this information directly when you describe "artificially disturbance".

We will add to the description of the DISCOL experiment, where we first mention the artificial disturbance in the methods section: ‘The DISCOL experiment was designed to artificially disturb the surface sediment layer ***by mixing*** *and removing nodules from the surface with a specially designed device, the so-called plough-harrow (Thiel and Schriever, 90 1990).’*
This way it is clarified what kind of disturbance we mention here and can later be better contrasted to the disturbance created by the epibenthic sledge as described in Line 97.

Line 115: 20 mictoliter of HCl was added to how much sample? 1 mL?

Yes, 1 mL. We will add this to the text: ‘ for 1 mL porewater’.

Line 116: “Additional sediment samples “. Do you mean a separate sediment core or the sediment leftovers after porewater extarction?

No, these variables were measured from the same core and sediment intervals. For porosity a few ml of wet sediment were taken, POC was measured from this subsample as well, and part of the squeeze cake after porewater extraction was used for radiometric analysis.

Line 119: you also show measured manganese data so you should add this to the list.

We do not show solid manganese data and dissolved manganese data is mentioned as part of the sentence ‘[…] for analysis of metal cations […]’ in Line 116.

Line 119-124: Can you add the sample sizes to this paragraph or add this in Table 2.

We will add the following sentence to Line 120: '1.3 mL of freshly extracted untreated pore water was diluted 3-fold before analysis.'

Line 154: Can you add equation numbers to all equations? That makes it easier to refer to them in the text.

We will add equation number to all equations in the text.

Line 176: shortly describe how the gridsize is distributed.

We will add to the existing information in brackets the following information: '(1D uneven grid ***with a sigmoidal distribution ranging from 0.1 cm at the surface and 1 cm at the lower boundary****)*

Line 178: describe that you use organic matter with different reactivities (Multi G approach) and give references for this approach (Jørgensen, 1978;Westrich and Berner, 1984; Middelburg, 1989).

We will add the following sentence to Line 180: 'To account for different reactivities of the various organic matter phases, we apply a 3G model (Jørgensen, 1978;Westrich and Berner, 1984; Middelburg, 1989) allowing for a labile, moderately reactive and a refractory phase.

Line 195: I do not see a sharp drop in porosity in figure 5.

Porosity decreases from 0.94 to 0.86 within the upper 10 cm and relative to the remaining core section, where porosity changes are only minimal, this decrease is indeed strong.
We will replace 'sharp' with 'significant'.

Line 195: You should also give the reference to the figure.

We will add a reference to the Figure.

Line 195: "and is rich in manganese". Can you add a concentration to this statement, or a range of concentrations.

We will add '1- 2 wt%' to the reference.

Line 200: "Organic carbon content in the DEA region oscillates about a mean value of 0.5 to 0.75 wt% in the upper 50 cm,". refer to figure.

We will add a reference to the figure

Line 202: "With depth the organic carbon content decreases steadily to about 1 wt% at 10 m.b". Add figure reference. Maybe I'm not looking at the right figure but the organic carbon content in fig 3 decreases to almost 0 and is never above 1 wt%.

Yes, this is a typological mistake, it should be 0.1 wt%!

Line 203-207: This part seems more suitable to the discussion. I think it is better to first discuss the data you show in figures 3-6.

We have divided the results section into (i) the description of the sediment and (ii) the description of the porewater. In the description of the sediment, sediment properties as well as composition of the sediment is included. Manganese nodules were found in the sediment core and their existence has to be mentioned here as well. We do not further discuss the implications of buried manganese nodules in this paper, because it is irrelevant for the research aims at hand. The authors would thus prefer to mention their existence only in the context of the core description.

Line 208-210: This is discussion, focus on presenting the data first.

As described in a previous response, we believe that the paper benefits from including well established zones of organic matter degradation processes in the description of the results.

Line 217: "Dissolved manganese is strongly redox sensitive and is absent in the upper oxic zone." Add reference to such a statement.

We will add a reference to Figure 4.

Line 226-228: Where can I see this Fe data? If you don't want to add this to the manuscript you can add it in an appendix.

As mentioned in a response above. The visualization of data that is below the detection limit is fruitless and a statement in the text should suffice. We will add the detection limit of 1 µmol/L to the text to clarify the upper boundary of dissolved Fe.

Lines 231-235: I would add this part to the methods.

The method section already includes all relevant information on the model. Keeping in mind that the first aim of this paper is an updated diagenetic model, the results section 'Diagenetic reference model' should include, in addition to the biogeochemical model results, a brief report on the success of this updated geochemical model. The introductory paragraph does exactly that; it states (i) that the 3G model allowed for a better model fit of the organic matter phase and (ii) that we were able to update information on bioturbation based on the new radiometric model presented in this paper. We would thus like to keep this paragraph in the results section.

Line 238: There should be a dot after inhomogeneities, Not a comma.

This will be amended.

Line 241: Can you further explain why you choose these sites?

We will add to Line 241: 'A satisfactory background model fit to undisturbed reference sites could be achieved […]'

Line 248: "which suggests that secondary reactions, such as a semi-labile Fe(II)-

oxygen reaction front, additionally shape the oxygen profile:" Why is this reaction not added in the model?

As mentioned in the following sentence, running the background model as a transient state adds a complexity to the model that we are not able to parameterize. Long term changes in organic matter input likely create changes in the oxygen penetration depth, which in turn will be buffered (only at first!) by the Fe(II)-O2 reaction layer. The fact that the oxygen profile is less curved as we expect, can indeed be an indicator, that organic matter input is slowly waning at present, allowing the oxygen penetration depth to gradually migrate downwards, where it burns down the Fe(II)-O2 layer, creating this more linear profile. Trying to parameterize this transient state will not benefit the prognostic impact simulation and will not benefit the paper.

Line 260: "relevant information" is a bit vague.

We will delete 'relevant'.

Line 264-266: Is this data compared to the reference stations?

Yes, we will add 'compared to the reference sites'.

Line 268: "signs of bioturbation are lacking". how would you see these and are these sign visible at the reference site?

*The physical expression of bioturbation, or lack thereof, in the sediment core is described in detail in the referenced paper. We will add more information to the text: ' […] **physical** signs of bioturbation (**recent bioturbation channels connected to the surface**) are lacking […].'*

Line 278: Can you give macrofaunal density (add a number).

1) The text says Megafauna – indeed as the reviewer suggests with his/her question, this should be macrofauna.

2) The observation in is based on 3D computed tomography scans – not on macrofauna densities. Specifically, the Vonnahme et al. analyzed whether the observed bioturbation channels extended all the way to the sediment surface (i.e., they are in use/recent) or not (i.e. they are likely abandoned/relict). Some likely recent bioturbation channels have been observed in the depressions created by the plough harrow (and to a lesser extent in the elevations/ridges). In the areas where deeper sediments were exposed at the surface, recent channels were missing. These observations have not been quantified by Vonnahme et al. (e.g., in terms of burrows / m^-2)

Line 292-295: These lines are repetition. This is already discussed in the introduction.

We will delete the introductory sentences: 'Oxygen is essential to all multicellular life and represents the electron acceptor with the highest energy yield. It exerts an important control on the sediment redox zonation and associated reactions (most importantly the oxic respiration of organic matter), which in turn control the distribution of other nutrients, such as ammonium and nitrate.'

Lines 300-304: For me it is difficult to understand how these changes were modeled. Can this be explained in the method section in more detail?

We will add to the methods section in Line 182 a paragraph on the transient model: 'Initial profiles of the transient simulations are based on the steady state background model which were adjusted for the modelled impact type: (i) in the case of 'sediment removal', the top 10 cm of the background profiles were cut off while maintaining bottom water concentrations and organic matter flux for the upper boundary conditions. For the 'sediment mixing' case, the oxygen concentrations of the upper 10 cm of the sediment were set to bottom water values, imitating an oxygen flooding event. Transient models were augmented by an additional Fe(II) profile - an oxygen reaction layer (Figure 2) - as justified by the surprisingly constant oxygen penetration depth at the reference and all disturbed sites. This Fe(II) reaction layer is crucial in the prognostic simulations which would otherwise predict that oxygen rapidly diffuses into deeper sediments after a disturbance event. It is assumed that bioturbation is inhibited immediately after the impact with a linear increase to undisturbed reference bioturbation intensity within 100 to 200 years.

And we will delete the sentences of Lines 300-304.

Line 305: "It is assumed that bioturbation is inhibited immediately after the impact with a linear increase to undisturbed reference bioturbation intensity within 100 to 200 years". Where is this assumption based on, can you give a reference?

We will add to the sentence '[…], which is in line with macrofaunal abundance data presented in Stratman et al., 2018.'

Line 311: "Upper centimetres". Give a number.

*We will add: 'restricted to the upper **10** centimetres'*

Line 321: For me it is quite surprising that there is such a large difference in such a short period.

Yes indeed, the bioturbation has a surprisingly strong influence on the redox zonation of the shallow sediment. If labile organic matter is only degraded right at the surface, where oxygen is easily replenished, oxygen can migrate much deeper into the sediment. If however, through bioturbation labile organic matter is transported deeper into the sediment, oxic respiration also occurs at sediment depth where oxygen is only replenished by diffusion which is much less efficient and thus downward oxygen migration is much more limited. This is why we can notice a difference if bioturbation recovery takes 200 years instead of 100 years.

Line 346: "overall surface fluxes vary". Where can I see the all the fluxes besides oxygen?

As mentioned in a previous response, we will add nitrate and ammonium fluxes to Figure 12.

Line 367 (Discussion): first paragraph does not give any new information or does discuss the results found in this study. The discussion reads as a summary/conclusion.

The first paragraph of the discussion is the only place where we describe in brief the balanced interplay between the physical, chemical and biological factors that shape the benthic ecosystem. This information is vital when discussing the ecosystem recovery after an impact that affects all ecosystem compartments. While the information therein is not novel to this study, to highlight the essential feedbacks between microbial/macrofaunal abundances and geochemical fluxes is the substance of the paper and is reflected in the data presented as well as in the modelling.

Line 370: "The associated microbial growth". Add references

The transfer of organic matter to microbial biomass has been demonstrated and quantified by pulse chase experiments with stable isotope-labeled organic matter in deep waters, including Pacific nodule provinces. Several experimental as well as modeling studies also show that this organic matter is subsequently used by metazoans. We will add references to the text: '[…] The degradation of organic matter is microbially catalyzed and in turn provides nutrients to the microbial community (e.g., Witte et al. 2003a, Moodley et al., 2005, Stratmann et al., 2018, Sweetman et al., 2019). The associated microbial growth provides biomass that sustains meio and macrofauna and forms an important component of the benthic food web (Witte et al., 2003b, van Oevelen et al., 2006, 2011). […]'

Moodley, L., Middelburg, J. J., Soetaert, K., Boschker, H. T. S., Herman, P. M. J., and Heip, C. H. R. (2005) Similar rapid response to phytodetritus deposition in shallow and deep-sea sediments, J. Mar. Res., 63: 457–469, https://doi.org/10.1357/0022240053693662

Stratmann, T., Mevenkamp, L., Sweetman, A. K., Vanreusel, A., van Oevelen, D. (2018) Has Phytodetritus Processing by an Abyssal Soft-Sediment Community Recovered 26 Years after an Experimental Disturbance? Front. Mar. Sci. 5:59, doi: 10.3389/fmars.2018.00059

Sweetman, A. K., Smith, C. R., Shulse, C. N., Maillot, B., Lindh, M., Church, M. J., ... Gooday, A. J. (2019). Key role of bacteria in the short-term cycling of carbon at the abyssal seafloor in a low particulate organic carbon flux region of the eastern Pacific Ocean. Limnology and Oceanography, 64(2), 694-713. https://doi.org/10.1002/lno.11069

Van Oevelen, D., Moodley, L., Soetaert, K., & Middelburg, J. J. (2006). The trophic significance of bacterial carbon in a marine intertidal sediment: Results of an in situ stable isotope labeling study. Limnology and Oceanography: 51: 2349-2359.

van Oevelen, D., Bergmann, M., Soetaert, K., Bauerfeind, E., Hasemann, C., Klages, M., Schewe, I., Soltwedel, T., Budaeva, N. E. (2011) Carbon flows in the benthic food web at the deep-sea observatory HAUSGARTEN (Fram Strait), Deep-Sea Research I 58: 1069-1083

Witte, U., Aberle, N., Sand, M., and Wenzhoefer, F. (2003a) Rapid response of a deep-sea benthic community to POM enrichment: an in situ experimental study, Marine Ecology-Progress Series 251: 27-36

Witte, U., Wenzhoefer, F., Sommer, S., Boetius, A., Heinz, P., Aberle, N., Sand, M., Cremer, A., Abraham, W. R., Jorgensen, B. B., Pfannkuche, O. (2003b) In situ experimental evidence of the fate of a phytodetritus pulse at the abyssal sea floor, Nature 424: 763-766

Line 379: "..infauna new material for additional degradation and microbial colonization,

close the causal cycle." Add reference

By means of stable isotope-labeled organic matter, several studies showed the downward mixing of organic matter and its use by microorganisms. We will add references to the text: '[…] Bioturbation plays thus a deciding factor in early-diagenetic, especially redox sensitive, processes. These are typically closely linked to the microbial functions and with the introduction of fresh and digested organic matter at depth by infauna new material for additional degradation and microbial colonization, close the causal cycle (Levin et al., 1997, Witte et al. 2003a, Middelburg, 2018) […]'.

Levin, L., Blair, N., DeMaster, D., Plaia, G., Fornes, W., Martin, C., Thomas, C. (1997) Rapid subduction of organic matter by maldanid polychaetes on the North Carolina slope, J. Mar. Res., 55, 595-611

Middelburg, J. J.: Reviews and syntheses: to the bottom of carbon processing at the seafloor, Biogeosciences, 15, 413–427, https://doi.org/10.5194/bg-15-413-2018, 2018

Witte, U., Aberle, N., Sand, M., and Wenzhoefer, F. (2003a) Rapid response of a deep-sea benthic community to POM enrichment: an in situ experimental study, Mar. Ecol.-Prog. Ser., 251: 27-36

Lines 386-388:" through changing the physical characteristics of the sediment surface, i.e. by exposing more compacted sediments with increased shear strength, and removing manganese nodules as hard substrate habitats." Add reference.

We will add the reference to this sentence: Grupe, B., H. J. Becker, and H. U. Oebius. 2001. Geotechnical and sedimentological investigations of deep-sea sediments from a manganese nodule field of the Peru Basin. Deep-Sea Res, Part II. 48: 3593–3608. doi:10.1016/S0967-0645(01)00058-3

Line 389: Where can I find the biological data?

Throughout the text microbial abundances are quoted and set into the context of biogeochemical processes. Also, Figure 12 presents referenced microbial and macrofaunal data.

Table 4:
"Number of points in the numerical grid (uneven)". How are they distributed?

As mentioned in a response to a previous comment, we will add a description of the uneven grid to the text: : '(1D uneven grid ***with a sigmoidal distribution ranging from 0.1 cm at the surface and 1 cm at the lower boundary****)*

- "Rate constant for reaction of Mn2+ and NO3". This equation is not given in table 3

This is an artefact from a previous manuscript version and should have been deleted. We found that this reaction does not play a significant role in our setting and set it to zero. This kinetic constant will be removed from the Table 3.

- How do the rate constants (last column) compare with values used in the literature? Are they in the same range? I think it would be good to add a column which described the ranges of rate constants used in the literature (with references).

Unfortunately, comparing kinetic constants is not very straight forward. We have tried to find suitable publications on comparable reaction rates for the organic matter degradation (e.g. Boudreau, 1996 in Computers and Geosciences, 22, p. 479 or Haeckel et al, 2001 in Deep-Sea Research II, 48, p. 3713 or Wang and Van Cappellen, 1996, in GCA, 60, p.2993), but different modelling approaches (e.g. 2G versus 3G) means that the kinetic constants cannot be compared. Also, secondary reactions strongly depend on the reaction network of the model and thus cannot be compared in a meaningful way.

There is no rate constant describing the third secondary reaction (oxidation of Fe2+)

We will add the kinetic rate constant for the Fe(II)-O2 reaction to Table 4 (1e2 mmol^-1 a^-1)

"Monod constant for SO42- reduction". This reaction is not in table 3. If you add this reaction you should also add Fe reduction coupled to organic matter.

SO4-reduction through organic matter degradation does not play a role at this site and we will thus remove it from Table 4.

Figure 8:

Total Corg. Not a very good fit. You could add more refractory OM deposition during the glacial periods.

Porewater profiles in the upper half meter or so (Einstein-Smoluchowski relation) are defined by Holocene POC input and hence, it adds no further value to play around with past temporal changes of POC input during glacial times. Indeed, a better fit could be achieved if we would temporally correlate the refractory organic matter input with glacial/interglacial intervals. For the purpose of this impact orientated paper, the labile and semilabile organic matter fraction are by far more important and can be sufficiently well represented by our steady-state model.
We will add in the description of the organic matter profile in Line 245:
'It should be noted that the geochemical state of the Peru basin is likely transient in nature arising from long-term (glacial/interglacial) as well as short-term (ENSO time scale) variations in the depositional flux of organic matter (König et al., 2001). ***This work focuses on modelling the biogeochemical processes in the upper half meter of the sediment, which are defined by the Holocene organic matter input, and are thus unaffected by long-term changes in the depositional flux****.'*

Also I would like to see how the three fractions are distributed with depth

We will add another window to Figure 8 where the three different OM fractions will be plotted.

For me it is unclear why/how the selection of stations is
made to fit the model. The stations are both inside and outside the DEA region.

In addition to the three designated reference stations we have also included two other undisturbed sites that were sampled during the cruise to complete the picture of the DEA area. This provides a better idea on the range of data scatter that can be expected from the DEA sites, especially with respect to the onset of dissolved manganese increase, for example.
We will add this information to the Figure caption of Figure 8:

'Simulation of background biogeochemical processes and their effect on solute profiles in the DEA region. ***In addition to the three reference stations, two other undisturbed sites were included for comparison.*** *See Table 4 for parameterization of the modelled profiles.'*

Figure 10
FeII2: Why not show the steady state? I think it would be better to use the same type of line for impact in all the plots.

We will add the Fe(II) steady state profile to Figure 10, which simply shows that the semi-labile Fe(II) reaction layer commences just below the O2 penetration depth, which is regulated by the present day organic matter input. Semi-labile Fe(II) that was present within the oxygenated zone has been 'burned down'.

Response to interactive comment on "DISCOL experiment revisited: Assessing the temporal scale of deep-sea mining impacts on sediment biogeochemistry" by Laura Haffert et al.

Anonymous Referee #2
Haffert and co-authors present a comprehensive sedimentary geochemical dataset on an experimentally disturbed potential deep-sea mining area, called DISCOL. The paper reports an extensive set of downcore geochemical data (O2, organic C, nutrients) from both short (MUC, box corer) as well as long (GC) cores in the experimental site. Further, the study improves an existing diagenetic reaction-transport model with datadriven process optimisations. The authors then use these new data plus transient early diagenetic simulations to asses the short and long-term impact of sediment removal during (future) mining of polymetallic nodules. They find that the removal of the surface labile organic carbon along with the nodules is the single most important driver of the establishment of a new geochemical regime in the disturbed areas.

The primary strength of this work is a quite convincing set of predictions as to what will happen in the long run when these nodules will be extracted from the seabed. The transient simulations are very useful and well integrated to the data. Supported by an extensive and novel dataset and the improved modelling approach, the integrated methodology could be used in other seafloor resource extraction scenarios as well. There is no significant weakness in the manuscript. It is well laid out and well written. I only have a few suggestions for a minor revision of the existing manuscript:

Overall comment: How does the Fe(II)-rich clay layer can trap nitrate? The redox reaction between the two is not that well established, and wondering if a more complex

cycle is present here, involving nitrogen intermediate species and a more complicated Fe(II)-Fe(III) cycle. I would propose that Figure 2 can be improved to clarify this, and both introduction (L84) and discussion parts can be expanded with a more detailed proposition of redox pathways.

The Fe(II)-rich layer in the Peru basin was discussed in detail in previous publications (König et al., 1997; König et al., 1999; König et al., 2001). Intermediate complexes where not discussed in this context, instead changes in the deposition flux of organic matter has caused a 'redox pump mechanism'. Figure 2 summarizes the findings for the DEA region. It should be kept in mind that the NO3 burn down of the Fe(II)-rich layer, which occurs at present at much greater depth, does not play a role for the research question at hand. We would thus like to avoid a detailed discussion on the Fe(II)-Fe(III) cycle and focus on the shallow sediments directly affected by potential mining activities.

L27: JPI Oceans - with plural 'oceans', I think is the right acronym.

Yes. We will correct this.

L54: the work 'untypically' can be removed without a significant change in the meaning of the sentence.

We will remove 'untypically' from the L54.

L58: 'availability positions' - perhaps could be re-phrased using 'order of the electron acceptors' or similar.

The sentence is trying to say that the redox zones are controlled by the availability of the various electron acceptors. To clarify the sentence we will change it to: 'The reactions utilize different terminal electron acceptors in the order of decreasing free-energy production, namely oxygen, nitrate, manganese oxide, iron oxide and sulphate and their availability controls the position of the various redox zones in the sediment column.'

Section 1.1 - overall I find this section is more like a discussion, rather than introduction. As mentioned above, the introduction of a Fe(II)-NO3 redox pathway is a little bit out of place in this section. Besides, the readers might expect a following section of 1.2, since there is 1.1, bot there is no other subsection of the introduction. Please consider re-organizing the material in 1.1.

In line with comments from Referee #1, we will restructure the information in the introduction. We will move the section, which intends to justify the introduction of a shallow Fe(II)-O2 reaction layer, to the description of the diagenetic model to Line 180:

L200-205 - interesting - did all cores include such buried nodule layers? I would strongly recommend to indicate the depth of these layers in the Figures 3-6 to be able to see directly in the figure if the nodule is impacting the geochemical profiles.

About half of the gravity cores included buried nodules. We will add the depth of manganese nodules to the gravity core profiles in Figure 3.

DISCOL experiment revisited: Assessing the temporal scale of deep-sea mining impacts on sediment biogeochemistry

Laura Haffert[1], Matthias Haeckel[1], Henko de Stigter[2] and Felix Janssßen[3]

[1] GEOMAR Helmholtz Centre for Ocean Research Kiel, Wischhofstrasse 1-3, 24148 Kiel, Germany

[2] NIOZ - Royal Netherlands Institute for Sea Research and Utrecht University, P.O. Box 59, 1790 AB Den Burg - Texel, The Netherlands

[3] HGF MPG Group for Deep Sea Ecology and Technology at the Max Planck Institute for marine Microbiology, Bremen and Alfred Wegener Institute Helmholtz Centre for Polar and Marine Research, Bremerhaven, Germany Max-Planck Institute for marine Microbiology, Bremen, Germany

Correspondence to: Laura Haffert (lhaffert@geomar.de)

Abstract. Deep-sea mining for polymetallic nodules is expected to have severe environmental impacts because in addition to the nodules, benthic fauna as well as the upper reactive sediment layer is removed through the mining operation, and blanketed by resettling material from the suspended sediment plume. This study aims to provide a holistic assessment of the biogeochemical recovery after a disturbance event by applying prognostic simulations based on an updated diagenetic background model and validated with novel (micro)-biological data. It was found that the recovery strongly depends on the impact type; complete removal of the reactive surface sediment reduces ~~seafloor nutrient fluxes~~benthic release of nutrients over centuries, while geochemical processes after resuspension and mixing of the surface sediment are near pre-impact state one year after the disturbance. Furthermore, the geochemical impact in the DISCOL area would be mitigated to some degree by a clay-bound Fe(II)-reaction layer, impeding the downward diffusion of oxygen, thus stabilizing the redox zonation of the sediment during transient post-impact recovery. The interdisciplinary (geochemical, numerical and biological) approach highlights the closely linked nature of benthic ecosystem functions, e.g. through bioturbation, microbial biomass and nutrient fluxes, which is also of great importance for the system recovery. It is, however, important to note that the nodule ecosystem may never recover to pre-impact state without the essential hard substrate and will instead be dominated by different faunal communities, functions and services

1 Introduction

This work is part of the JPI Oceans MiningImpact project, which is an integrated research project assessing the potential ecological impact caused by dee-sea mining for polymetallic nodules. Most of these nodules occur in the deep ocean basins at water depths greater than 4000 meter, which represents a part of the ocean that is largely unstudied. In fact, until recently it was assumed that life would be sparse in the deep ocean where, in the absence of light, the only energy source is falling organic matter produced in the photic zone. Increased research interest and technological advances to overcome the large distances and pressure differences of over 400 times the atmospheric pressure have revealed that the deep-sea hosts a surprising diversity of life forms. Information on benthic ecosystem functions, including spatial heterogeneity, temporal variability, and biogeochemical

feedbacks are still limited, but are an important prerequisite in the evaluation of the environmental impacts of deep-sea mining.

This work focuses on a unique study area in the Peru basin (Figure 1), where in 1989 a circular area with a diameter of about 2 nautical miles was intensely disturbed with a plough-harrow as part of the DISturbance and ~~recolonization~~ reCOLonization experiment (DISCOL) (Thiel and Schriever, 1990). The DISCOL experimental area (DEA) was revisited before and several times after the initial disturbance, with research concentrating mainly on the characterization and distribution of benthic fauna (Borowski and Thiel, 1998) (Borowski and Thiel, 1998; Borowski, 2001; Bluhm, 2001). Macrofaunal communities, which are particularly important for the bioturbation and thus redox zoning of the sediment, are mainly composed of Polychaeta (about 50%) and to a lesser extent tanaidacea (10 - 20%) and bivalvia (5 – 10%) (Borowski and Thiel, 1998). After the artificial disturbance, very few faunal groups returned to baseline or control conditions after more than two decades (Jones et al., 2017) and the main mode of macrofaunal recolonization was found to be via lateral migration (Borowski and Thiel, 1998).

~~(Borowski and Thiel, 1998); Borowski (2001).~~ The current MiningImpact project makes use of the technological advances that have taken place in recent years, e.g. precise underwater positioning and in-situ experimentation by remotely operated vehicles (ROVs), in situ oxygen measurement, precise sampling with TV-guided or ROV manipulated equipment and analysis of microbial functions, and attempts to derive a holistic understanding of the deep-sea mining impact on the closely linked ecosystem functions. The specific objectives of this work are:

(i) Creating a biogeochemical (diagenetic) reference model for the DEA region and validating it based on a comprehensive set of geochemical data (pore water and solid phases from undisturbed and disturbed sediments) obtained with state-of-the-art ~~geochemical dataset~~methodology ~~(pore water and solid phase) on both undisturbed and disturbed sediments~~.

(ii) Determining short to long-term impacts of a deep-sea mining event on the geochemical system through field data supported simulations.

(iii) Advancing our understanding on the intricate interplay between ecosystem functions and geochemical processes in the context of a benthic disturbance in the deep sea.

~~**1.1 Biogeochemistry of the Peru Basin**~~

~~In comparison to other abyssal areas, the Peru basin receives untypically high organic matter input, which is fueled by the equatorial high productivity zone (Weber et al., 2000). The degradation of deposited organic matter plays a crucial role in defining the benthic biogeochemical system (Froelich et al., 1979). The reactions utilize different terminal electron acceptors in the order of decreasing free energy production, namely oxygen, nitrate, manganese oxide, iron oxide and sulphate and their availability positions the various redox zones in the sediment column. König et al. (1999), König et al. (2001) and Haeckel et al. (2001) have previously identified and quantified through diagenetic modelling the main biogeochemical processes in the Peru Basin, including the DEA region. They found that organic matter degradation progresses through the stages of oxic respiration, denitrification and manganese reduction before the reactive fraction of organic matter is diminished leaving only the most refractory fraction of organic material to be permanently buried. A large quantity of organic matter is degraded by oxic respiration in a surface 'reaction layer' which is bounded by the bioturbation depth at the lower end. Oxygen is depleted at a sediment depth of 5 to 15 cm, with the DEA region being on the deeper end.~~

Formatted: Highlight

Formatted: Highlight

Formatted: Highlight

Formatted: Highlight

~~Larger variations were found among the nitrate profiles. In the slightly shallower region of the Peru Basin seawater-derived nitrate and nitrate from oxic respiration is consumed within the bioturbated upper 20 cm of sediment. In contrast, in the DEA region nitrate escapes the reaction layer and diffuses to a depth of about 2 m, where a Fe(II) rich reaction layer impedes further downward migration (König et al., 2001; see also Figure 2). This reaction layer was formed during glacial times, when organic matter deposition was strongly increased and potential electron acceptors such as oxygen, nitrate and manganese oxide were exhausted closely below the sediment surface. During these times, structural Fe(III) within smectite lattices acted as the thermodynamically favored electron acceptor, creating Fe(II) rich surface sediments that were subsequently buried (Lyle, 1983). This process was reversed when waning organic matter input during interglacial periods allowed oxygen and nitrate to migrate downwards thus creating a 'burn-down' situation of the redox sensitive Fe(II) rich smectite phase (Figure 2). The position of the reaction front is easily distinguished in deep sediment cores as a transition from a tan to green color change (Lyle, 1983) and has also been confirmed by Mössbauer spectroscopic measurements.~~(Drodt et al., 1997; König et al., 1997; König et al., 1999)~~.~~

~~Comparatively little is known about the redox potential of Fe(II) on different crystallographic lattice positions (coordination sites) in clay minerals, such as nontronite. In particular, information is lacking on the reactivity of the Fe(II) on these sites with respect to oxidation by nitrate and oxygen. Available Mößbauer data (König et al., 2001) from the DISCOL area indicates a refractory fraction of Fe(II) that prevails in the nitrate reduction zone (~10 % of total iron). We propose that part of this refractory fraction is in fact semi-labile and that oxygen, which has a higher redox potential than nitrate, can oxidise this semi-labile Fe(II) and thus presents a second reaction front impeding the downward migration of oxygen.~~

2 Methods

~~1.1 Biogeochemistry of the Peru Basin~~Biogeochemical site description

In comparison to other abyssal areas, the Peru basin receives ~~untypically~~ high organic matter input, which is fueled by the equatorial high-productivity zone (Weber et al., 2000). The degradation of deposited organic matter plays a crucial role in defining the benthic biogeochemical system (Froelich et al., 1979). The reactions utilize different terminal electron acceptors in the order of decreasing free-energy production, namely oxygen, nitrate, manganese oxide, iron oxide and sulphate and their availability controls the position of the various redox zones in the sediment column.~~The reactions utilize different terminal electron acceptors in the order of decreasing free-energy production, namely oxygen, nitrate, manganese oxide, iron oxide and sulphate and their availability positions the various redox zones in the sediment column.~~ König et al. (1999), König et al. (2001) and Haeckel et al. (2001) have previously identified and quantified through diagenetic modelling the main biogeochemical processes in the Peru Basin, including the DEA region~~:~~. They found that organic matter degradation progresses through the stages of oxic respiration, denitrification ~~and~~, manganese and in deeper sediments iron oxide reduction before the reactive fraction of organic matter is diminished leaving only the most refractory fraction of organic material to be permanently buried. Unlike manganese, the reduced Fe^{2+} species is not released into the porewater but instead incorporated into the clay mineral phase as nontronite resulting in dissolved Fe concentrations below or near detection limit. ~~A~~The largest quantity of organic matter is degraded by oxic respiration in a surface 'reaction layer' which is bounded by the bioturbation depth at the lower end.

Field Code Changed

Formatted: Highlight

Formatted: Highlight

Field Code Changed

Field Code Changed

Formatted: Superscript

Oxygen is depleted in the Peru Basin at a sediment depth of 5 to 15 cm, with the DEA region being on the deeper end (Haeckel et al., 2001). Larger variations were found among the nitrate profiles. In the slightly shallower region of the Peru Basin seawater-derived nitrate and nitrate from oxic respiration is consumed within the bioturbated upper 20 cm of sediment. In contrast, in the DEA region nitrate escapes the reaction layer and diffuses to a depth of about 2 m, where a Fe(II)-rich ~~reaction~~ layer impedes further downward migration (König et al., 2001; see also Figure 2). This Fe(II)-rich ~~reaction~~ layer was formed during glacial times (corresponding to an age of at least 60 ka), when organic matter deposition was strongly increased and potential electron acceptors such as oxygen, nitrate and manganese oxide were exhausted closely below the sediment surface (König et al., 2001). During these times, structural Fe(III) within smectite lattices acted as the thermodynamically favored electron acceptor, creating Fe(II)-rich surface sediments that were subsequently buried (Lyle, 1983). This process was reversed when waning organic matter input during interglacial periods allowed oxygen and nitrate to migrate downwards thus creating a 'burn-down' situation of the redox sensitive Fe(II)-rich smectite phase (Figure 2). The position of the reaction front is easily distinguished in deep sediment cores as a transition from a tan to green color change (Lyle, 1983) and has also been confirmed by Mössbauer spectroscopic measurements (Drodt et al., 1997; König et al., 1997; König et al., 1999).

Comparatively little is known about the redox potential of Fe(II) on different crystallographic lattice positions (coordination sites) in clay minerals, such as nontronite. In particular, information is lacking on the reactivity of the Fe(II) on these sites with respect to oxidation by nitrate and oxygen. Available Mößbauer data (König et al., 2001) from the DISCOL area indicates a refractory fraction of Fe(II) that prevails in the nitrate reduction zone (~10 % of total iron). We propose that part of this refractory fraction is in fact semi-labile and that oxygen, which has a higher redox potential than nitrate, can oxidise this semi-labile Fe(II) and thus presents a second reaction front impeding the downward migration of oxygen.

Formatted: Highlight

Formatted: Highlight

Field Code Changed

Formatted: Normal

2.1 Disturbance experiments

The current study presents information collected in the DEA during the two legs of the SO242 research cruise in 2015. The DISCOL experiment was designed to artificially disturb the surface sediment layer through mixing and remove nodules from the surface with a specially designed device, the so-called plough-harrow (Thiel and Schriever, 1990); To this end the ~4150 m deep circular DEA (11 km^2) was crossed 78 times starting from various directions resulting in a heavily disturbed area in the center and less disturbed peripheral regions. In total about 20% of the DEA was directly ploughed with the remaining 80% being not directly disturbed but – at least in part – covered by an up to 30 mm thick re-settled sediment blanket (Schriever and Thiel, 1992).

During the first leg of SO242 an additional artificial disturbance was created using an epibenthic sled (EBS) which was sampled 5 weeks later on the second leg of SO242. The epibenthic sled (CliSAP-Sled; Brenke (2005)) has a width of 2.4 m and weight of 880 kg (in air). Unlike the plough-harrow, which 'mixes' the upper sediment layer, the EBS largely scrapes off the upper centimetres of sediment (most of the reactive, bioturbated layer), including embedded nodules and bulldozes them sideways from the track.

2.2 Sampling procedure

A map of the sampling stations as well as a table of the exact positions are provided in Figure 1 and Table 1, respectively. Several devices were deployed at each sampling site to retrieve surface and subsurface sediment

samples (Greinert, 2015; Boetius, 2015): (i) a multiple-corer (MUC, Oktopus, Kiel, Germany), which samples the upper 20 – 40 cm of the sediment including the overlying bottom water; The corer was equipped with a TV-Camera system for precise positioning, e.g. for sampling specific seafloor features like the disturbance tracks; (ii) a ROV-deployed push-corer (PUC) focusing on small-scale topographic features created by the seafloor disturbance; (iii) a box-corer (BC - USNEL type; Hessler and Jumars, 1974) to sample the sediment including macrofauna and nodules; and (iv) a gravity-corer (GC) extracting sediment up to 10 mbsf.

After core retrieval the samples were brought into the ship's cold room (approx. 4 °C). 1 m long sections of the gravity cores were cut into two half cylinders dedicated for sampling and archiving. The working half of the gravity cores were sampled by extracting 3 cm thick slices at intervals of 20 to 40 cm. Sediment from the plastic liners of the other corers were extruded with a piston and cut into 0.5 to 2 cm thick slices under an oxygen-free, argon atmosphere in a glove bag. Subsequently, the pore water was extracted using a low pressure-squeezer (argon gas at 3-5 bar) and filtered through a Nuclepore 0.2 µm polycarbonate filter. Porewater extracted from the samples was stored in two recipient vessels: (i) an acidified sample (i.e. pH<1 with 20 µl 30% HCl suprapur per 1 ml sample) for analysis of metal cations and (ii) a non-acidified sample for nutrients. Additional sediment samples were collected from the same core and sediment intervals for porosity, organic carbon content and radiometric analysis.

2.3 Analytical methods

Analyses for the porewater solutes NO_3^-, NO_2^-, NH_4^+, PO_4^{3-}, SiO_4^{4-} ~~and Fe^{2+}~~ were completed onboard using a Hitachi UV/VIS spectrophotometer on 1.3 ml of freshly extracted untreated pore water which was diluted 3-fold before analysis. The respective chemical analytics followed standard procedures (Grasshoff et al., 1999), i.e. nitrite and nitrate (after reduction with Cd) were measured as sulphanile-naphthylamide, ammonium was measured as indophenol blue, phosphate and silicate as molybdenum blue, and iron with ferrospectral. The total alkalinity of the porewater was determined by titration with 0.02 N HCl using a mixture of methyl red and methylene blue as indicator. The titration vessel was bubbled with argon to strip any CO2 produced during the titration. The IAPSO seawater standard was used for calibration. Further details on analytical methods, e.g. analytical precision and accuracy, are given in Table 2.

At the NIOZ laboratory sediment profiles of ^{210}Pb and ^{226}Ra, radio-isotopes from the ^{234}U decay series were measured in multicores for determining biological mixing rates integrated over a ~100 year time-scale. Total ^{210}Pb and ^{226}Ra activity were determined directly by gamma-spectrometry, whilst total ^{210}Pb was also measured indirectly by alpha-spectrometry via its granddaughter isotope ^{210}Po. Activities of anthropogenic ^{137}Cs proved to be generally below detection level. Radionuclide activities are reported in the data base as mBq g^{-1} dry sediment.

For gamma-spectrometry, a few grams of freeze-dried and homogenized sediment sample was contained in a 5 cm diameter plastic petri dish, which was closed with tape and sealed gas-tight in a plastic envelope. After leaving the sample for at least 4 weeks to ensure equilibrium, measurement of ^{210}Pb and ^{226}Ra were undertaken with a Canberra Broad Energy Range High Purity Germanium Detector (BEGe), using the 46.5 keV line for ^{210}Pb and 295.2, 351.9 and 609.3 keV lines for ^{226}Ra. The detector, connected to a computer via a Digital Spectrum Analyser (DSA-1000), counted the radionuclide activities with Genie 2000 gamma spectroscopy software. The detector was externally calibrated with a Geological Certified Reference Material IAEA/RGU-1, with reference date of 01-01-1988. A monitor standard IAEA-300 provided quality control. Excess ^{210}Pb

activities were calculated by subtracting ^{226}Ra activity averaged for the 295.2, 351.9 and 609.3 keV lines from the measured total ^{210}Pb activity.

For alpha spectrometry measurement of ^{210}Po, 0.5 g of freeze-dried and homogenised sediment sample was spiked with 1 ml of a standard solution of ^{209}Po in 2M HCl, and then leached for 6 h in 10 ml of concentrated HCl heated to 85°C. After diluting the fluid with 45 ml of demineralised water and adding 5 ml of an aqueous solution of ascorbic acid (40 g L^{-1}), natural ^{210}Po and added ^{209}Po were collected from the fluid by spontaneous electrochemical deposition on silver plates. For subsequent alpha-spectrometry, Canberra Passivated Implanted Planar Silicon detectors were used. ^{210}Pb activity was calculated from ^{210}Po, assuming secular equilibrium and correcting for the time elapsed since collection of the samples.

2.4 Numerical methods

We follow the classical approach in early diagenetic modeling where partial differential equations represent the diffusive and advective fluxes coupled to a reaction term (R), as formulated by Berner (1980). When applying a conversion via the volume fraction, expressions for solutes and solids can be derived, respectively:

$$\frac{\partial \phi C_{pw}}{\partial t} = \frac{\partial}{\partial x}\left(\phi D \frac{\partial C_{pw}}{\partial x} - \phi\, u\, C_{pw}\right) - \phi R\left(C_{pw}\right) \quad \text{Eq.(1)}$$

~~$\frac{\partial \phi C_{pw}}{\partial t} = \frac{\partial}{\partial x}\left(\phi D \frac{\partial C_{pw}}{\partial x} - \phi\, u\, C_{pw}\right) - \phi R\left(C_{pw}\right)$~~

and

$$\frac{\partial (1-\phi) C_s}{\partial t} = \frac{\partial}{\partial x}\left((1-\phi) Db \frac{\partial C_s}{\partial x} - (1-\phi)\, w\, C_s\right) - (1-\phi) R(C_s) \quad \text{Eq.(2)}$$

~~$\frac{\partial (1-\phi) C_s}{\partial t} = \frac{\partial}{\partial x}\left((1-\phi) Db \frac{\partial C_s}{\partial x} - (1-\phi)\, w\, C_s\right) - (1-\phi) R(C_s)$~~

where t and x represent time and the depth under the seafloor, respectively; C_{pw} and C_s are the molar species concentration of solute or solid, respectively; ϕ is the porosity; u and w represent fluid and sediment velocity due to burial. Solute diffusion and sediment bioturbation is scaled by the effective diffusion coefficient D and the bioturbation coefficient Db.

The porosity-depth profile is assumed to be produced by steady-state compaction (Berner, 1980) and is approximated empirically by the following exponential function (Murray et al., 1978; Berner, 1980; Martin et al., 1991; Rabouille and Gaillard, 1991b, a):

$$\phi(x) = \phi_\infty + (\phi_0 - \phi_\infty)\, e^{-\beta x} \quad \text{Eq.(3)}$$

~~$\phi(x) = \phi_\infty + (\phi_0 - \phi_\infty)\, e^{-\beta x}$~~

where ϕ_∞ is the porosity at infinite depth, ϕ_0 is the porosity at the sediment surface (x=0) and β is the porosity attenuation coefficient.

The fluid and sediment velocity-depth distribution is calculated according to the mathematical convention of Luff and Wallmann (2003):

$$u(x) = \frac{\phi_\infty\, w_\infty}{\phi(x)} \quad \text{Eq.(4)}$$

Formatted: Left
Formatted Table
Formatted: Right

and

$$w(x) = \frac{1-\phi_\infty}{1-\phi(x)}\, w_\infty \qquad \text{Eq.(5)}$$

~~$u(x) = \frac{\phi_\infty w_\infty}{\phi(x)}$ and $w(x) = \frac{1-\phi_\infty}{1-\phi(x)}\, w_\infty$~~

where w_∞ is the burial velocity at infinite depth.

The effective diffusion coefficient was tortuosity corrected:

$$D\,(x) = \frac{D^o(x)}{\theta^2(x)} \qquad \text{Eq.(6)}$$

~~$D\,(x) = \frac{D^o(x)}{\theta^2(x)}$~~

with D_0 being the infinite dilution molecular diffusion coefficient calculated after Berner (1980) and θ^2 being the squared tortuosity. The tortuosity can be related to the porosity ϕ according to Boudreau (1996):

$$\theta^2(x) = 1 - 2\ln\phi(x) \qquad \text{Eq.(7)}$$

~~$\theta^2(x) = 1 - 2\ln\phi(x)$~~

The bioturbation profile is approximated by the arbitrary function:

$$Db = Db^0 \cdot 0.5\, erfc\left(\frac{x - x_{Db}}{\beta_{Db}}\right) \qquad \text{Eq.(8)}$$

~~$Db = Db^0 \cdot 0.5\, erfc\left(\frac{x - x_{Db}}{\beta_{Db}}\right)$~~

Where Db^0 represents the maximum bioturbation intensity at the sediment surface, x_{Db} is the bioturbation half depth and β_{Db} the bioturbation attenuation coefficient.

The diagenetic equations consisting of a set of partial differential equations (Equation 1 and 2), are solved via a finite difference scheme (1D uneven grid with a sigmoidal distribution ranging from 0.1 cm at the surface and 1 cm at the lower boundary) and subsequent minimization of the ordinary differential equations by inbuilt ODE solvers of MATLAB.

The reaction network shaping the geochemistry of the upper sediment metres, namely organic matter degradation and secondary redox reactions including the oxidation of ammonium and dissolved manganese, are listed in Table 3 as well as the corresponding rate expressions. To account for different reactivities of the various organic matter phases, we apply a 3G model (Jorgensen, 1978; Westrich and Berner, 1984; Middelburg, 1989) allowing for a labile, moderately reactive and a refractory phase. We also included a shallow semi-labile Fe(II) layer that reacts with oxygen to the model (Figure 2). While it is established that a labile Fe(II) reaction front impedes the downward migration of nitrate (König et al., 1997; König et al., 1999), little is known about the redox potential of Fe(II) on different crystallographic lattice positions (coordination sites) in clay minerals, such as nontronite. In particular, information is lacking on the reactivity of the Fe(II) on these sites with respect to oxidation by nitrate and oxygen. Available Mößbauer data (König et al., 2001) from the DISCOL area indicate a refractory fraction of Fe(II) that prevails in the nitrate reduction zone (~10 % of total iron). In the light of the much higher redox potential of oxygen compared to nitrate, we model the remaining Fe(II) as a semi-

Formatted: Font: 10 pt

Formatted: Highlight

labile phase representing a second reaction front impeding the downward migration of oxygen~~The reaction network shaping the geochemistry of the upper sediment metres, namely organic matter degradation and secondary redox reactions including the oxidation of ammonium, dissolved manganese and refractory clay bound Fe(II) are listed in Table 3 including the corresponding rate expressions~~. The diagenetic model is applied to define a background or reference geochemical system. This is then used to derive transient prognostic models in response to different impact types. Initial profiles of the transient simulations are based on the steady state background model which were adjusted for the modelled impact type: (i) in the case of 'sediment removal', the top 10 cm of the background profiles were 'cut off' while maintaining bottom water concentrations and organic matter flux for the upper boundary conditions. For the 'sediment mixing' case, the oxygen concentrations of the upper 10 cm of the sediment were set to bottom water values, imitating an oxygen flooding event. Transient models were augmented by an additional Fe(II) profile - an oxygen reaction layer (Figure 2) - as justified by the surprisingly constant oxygen penetration depth at the reference and all disturbed sites. This Fe(II) reaction layer is crucial in the prognostic simulations which would otherwise predict that oxygen rapidly diffuses into deeper sediments after a disturbance event. It is assumed that bioturbation is inhibited immediately after the impact with a linear increase to undisturbed reference bioturbation intensity within 100 to 200 years, which is in line with macrofaunal abundance data presented in Stratmann et al. (2018a). A detailed parameterization of the background and prognostic models is provided in Table 4.

The bioturbation coefficient Db^0-, a critical input parameter to the background model, is derived by fitting a simplified version of the background model to summed ^{210}Pb, ^{226}Ra and ^{230}Th radiometric data. The physical set up of the model is the same as the background model with the difference that only the above mentioned radiometric species and their first order radioactive decay is considered.

3 Results

3.1 Geochemistry of the DEA region

The parameter depth profiles for each core are presented in Figure 3 – 6, grouped in 'outside DEA' and 'inside DEA' stations for the gravity cores and for the multiple and box cores in reference sites and various types of disturbed sites.

Geochemical trends observed in the sediment cores from reference stations agree in general well with those observed in the same area during a previous investigation (Haeckel et al., 2001). The upper reactive sediment section (up to ~20 cm.b.s.f) is markedly different from the deeper sediment sections (up to 10 m) (Figure 3). It is characterized by a ~~sharp~~ significant decrease in porosity (from 0.94 to approx. 0.86, Table 4 and Figure 4) and is rich in manganese oxides (1 - 2 wt%, Paul et al., 2019), which gives this layer its distinct dark brown color. Below this layer, the sediment takes on a light brown to grey brown (tan) color, which is replaced by a grayish green color - the shift to Fe(II)-rich lattices in the smectite phase – at a depth of 2 – 2.5 m (38GC1, 84GC3, 100GC5, and 123GC6, Table 1). Organic carbon content in the DEA region oscillates about a mean value of 0.5 to 0.75 wt% in the upper 50 cm (Figure 3), which is controlled by the difference in organic carbon input during glacial (higher C_{org} content) and interglacial (lower C_{org} content) sedimentation regimes (Haeckel et al., 2001). With depth the organic carbon content decreases steadily to about 0.1 wt% at 10 m.b.s.f (Figure 3). Contrary to previous observations that nodules in the DEA area occur only at the sediment surface, investigation of the

Formatted: Not Highlight

current set of gravity cores revealed buried manganese nodules at depths of 4 to 8 m (Figure 3). The undisturbed appearance of the sediment surrounding these buried nodules, and evidence of diagenetic alteration of the nodules, proves that these nodules were genuinely buried and do not represent a coring artifact.

In situ oxygen profiles confirm that the upper brown layer represents the oxygenated zone (Figure 5~~6~~). In this zone, oxic respiration of organic matter not only consumes downward diffusing oxygen but increases ammonium and, via nitrification, also nitrate (Figure 6~~4~~). While the trend in the nitrate profiles is clearly discernable, ammonium concentrations remain rather low (10 – 20 µmol/l) and are scattered and are likely controlled by secondary processes, such as adsorption and desorption (Haeckel et al., 2001). Below the oxic dark brown layer, denitrification commences and nitrate declines within the upper 2 -3 m of the sediment and is entirely depleted in the cores with the greyish green Fe(II)-rich reaction layer (51GC2, 84GC3, 100GC5, 123GC6, Figure 3). The depleted nitrate profiles tend to be more linear (e.g. 84GC3) than the profiles of cores where the Fe(II)-rich layer is absent (e.g. 132GC7), as is typical in the presence of a reaction layer (Goloway and Bender, 1982; Wilson et al., 1985; Jahnke et al., 1989). Dissolved manganese is strongly redox sensitive and is absent in the upper oxic zone (Figure 6). Below the oxic zone, organic matter degradation progresses to manganese oxide reduction and produces dissolved manganese, which increases steadily until it reaches an asymptotic concentration at 6 m depth with terminal concentrations ranging between 25 and 120 µmol/l (Figure 3). Diagenetic simulations (Haeckel et al., 2001) could not reproduce this strong increase in dissolved manganese and the discovery of buried manganese nodules now confirms that the dissolved manganese concentrations are indeed additionally shaped by the dissolution of manganese nodules at a depth of 4 – 8 m.

Alkalinity profiles are largely unchanged over the entire sampling domain (up to 10 m), but display some variations in the upper 5 cm (Figure 6). Haeckel et al. (2001) have argued that the alkalinity profile is likely influenced by carbonate geochemistry, so we will neglect the upper alkalinity profile in our interpretations. Dissolved iron concentrations were near or below the detection limit of 1 µM in all cores due to its incorporation into the clay mineral phase and sulphate concentrations remained close to their sea water value, which is in line with the absence of ~~iron and~~ sulfate reduction in the Peru basin.

3.2 Diagenetic reference model

With the MiningImpact sampling campaign specifically targeting the DEA region, we were able to update the parameterization of the previous model presented by Haeckel et al. (2001). The main differences are: (i) The presented model applies a 3G-model, i.e. allows for three fractions of organic matter with varying reactivity, and thus a better fit to the field data. And (ii) The bioturbation intensity (D_B = 0.65) and depth profile are now based on radioactive disequilibria between radionuclides of the natural uranium and thorium series in the DEA region (Figure 7). The numerical simulations predict that excess ^{210}Pb (difference between solid and dashed lines) exists down to ~10 cm and below the measured activity is supported by ^{230}Th (dotted line) and ^{226}Ra (difference between dashed and dotted lines). A relatively high scatter of radioactive activities of 1.5-3 Bq/g was observed in the uppermost sediment samples (0-0.5 cm) reflecting lateral inhomogeneities~~.~~. These could be due to sediment focusing created by local topography, e.g. small depressions acting as deposition centers for fluffy material or by 'hotspots' of non-local mixing by individual organisms.

A satisfactory background model fit to undisturbed reference sites could be achieved for all relevant parameters with particular focus being placed on accurately simulating the redox zonation of the sediment, especially the oxygen penetration depth and the concurrent increase in dissolved manganese (Figure 8). It should be noted that

Formatted: Not Highlight

the geochemical state of the Peru basin is likely transient in nature arising from long-term (glacial/interglacial) as well as short-term (ENSO time scale) variations in the depositional flux of organic matter (König et al., 2001). This work focuses on modelling the biogeochemical processes in the upper half meter of the sediment, which are defined by the Holocene organic matter input, and are thus unaffected by long-term changes in the depositional flux. Similar to the downward migrating nitrate front, it is likely that the pore water oxygen content also increases with currently waning organic matter input. The analytical oxygen profiles display less curvature (more linearity) than the modelled profiles, which suggests that secondary reactions, such as a semi-labile Fe(II)-oxygen reaction front, additionally shape the oxygen profile. However, due to the uncertainty in a transient parameterization, we model the reference sediments as a steady state scenario - justified by the generally good agreement of the model with the geochemical data.

3.3 Impact characterization

All sample stations were affected by at least one of the following processes: (i) removal of the upper dark brown reactive layer, (ii) mixing and redistribution of the surface sediment resulting in piling up ('riges') and removal ('furrows'), (iii) turning of the upper sediment upside down or bringing up deep sediment to the surface – both leading to exposal of sediment from below the reactive layer at the surface and (iv) deposition of re-suspended sediment. Furthermore, there were distinct differences in the physical impact of the plough-harrow and EBS track. While the EBS scraped off the surface sediments and relocated them to the side of the track, the plough-harrow mixed and displaced sediments resulting in a variety of disturbance structures. In the following a detailed description of the physical and geochemical impact is provided and will be complemented by ~~relevant~~ information on the microbiological impact from a parallel study (Vonnahme et al., in press).

Sediments inside the EBS track are largely devoid of the upper reactive brown layer, exposing the tan-colored subsurface sediment in places. The surface of the track is smooth indicating that sediment mixing is negligible inside the tracks. Removal of the upper reactive layer resulted in decreased sediment porosity by exposing more compacted sediment compared to the reference sites and brought the boundary below which dissolved manganese is found in the sediment pore water as close as 5 cm bsf. (Figure ~~4~~ 4 and ~~5~~6). In contrast, the oxygen penetration depth does not vary significantly from the reference area, the profile shape is however slightly more linear (Figure ~~6~~5). In line with the severe disturbance of the sediment, physical signs of bioturbation (recent bioturbation channels connected to the surface) are lacking ~~signs of bioturbation are lacking~~ and the microbial cell count in the surface sediment is reduced by 50% with the microbial communities being significantly different from the reference sites (Vonnahme et al., in press).

The disturbance of the surface sediment layer brought about during the DISCOL experiment were still clearly visible after 26 years and the TV-guided sampling campaign was able to specifically target the following features: (i) The area next to the plough-harrow track ('outside track'), that is not mechanically disturbed but affected by resettling sediment from the disturbance plume. Geochemical profiles do not indicate a significant difference to the reference site (Figure ~~4~~6), especially with the natural heterogeneity of the area in mind. Differences in the microbial functions compared to the reference stations are also within the methods' confidence level and recent bioturbation confirms that the sediment is presently colonized by burying ~~megafauna~~ macrofauna (Vonnahme et al., in press). (ii) The furrows drawn in the seabed by the plough-harrow show some distinct differences to the reference sites. The reactive dark brown surface layer is reduced in thickness and is overlain by re-settling sediment which preferentially accumulated in the depression. While

geochemical profiles do not differ significantly from the reference site, biological processes are noticeably decreased (Vonnahme et al., in press). (iii) 'Ridge' sediments show the same disturbance effects, albeit more severe, and seafloor integrity is compromised by deep cracks throughout the sediment (Vonnahme et al., in press). (iv) Exposed subsurface sediment observable as lighter-coloured patches show the highest level of disturbance, similar in character to the fresh surface created by the EBS. The reactive brown layer is absent and thus the porosity of the surface sediment reduced (Figure 4~~5~~). Biological processes are significantly impacted. Bioturbation channels are scarce and disconnected with the surface, indicating a pre-impact origin. Microbial cell numbers are reduced by 30% with the microbial communities being more similar to those of the subsurface sediment (14-16 cm.b.s.f.) of the reference stations than those of the surface sediments (Vonnahme et al., in press).

3.4 Prognostic simulations

The following presentation of simulation results focuses on the distribution of oxygen, which plays a central role in biogeochemical processes: ~~Oxygen is essential to all multicellular life and represents the electron acceptor with the highest energy yield. It exerts an important control on the sediment redox zonation and associated reactions (most importantly the oxic respiration of organic matter), which in turn control the distribution of other nutrients, such as ammonium and nitrate.~~ Different impact types were simulated by two 'end member' scenarios. The first scenario assumes that 10 cm of the upper sediment were removed, i.e. the first 10 cm of the reference steady-state profiles were discarded, exposing anoxic subsurface sediments to bottom water concentrations. The second scenario floods the upper 10 cm of the sediment with oxygen, representing, on one hand, the effect of sediment mixing and cracking and, on the other, the effect of re-suspension and subsequent settling of freshly oxygenated reactive sediment (Figure 9). ~~Impact simulations use the steady state background model as initial profiles (adjusted for the modelled impact type, i.e. removing the upper 10 cm or setting oxygen concentrations to bottom water values) and augmented by an additional Fe(II) profile – an oxygen reaction layer (Figure 2) – as justified by the surprisingly constant oxygen penetration depth at the reference and all disturbed sites (Figure 6). This Fe(II) reaction layer is crucial in the prognostic simulations which would otherwise predict that oxygen rapidly diffuses into deeper sediments after a disturbance event (Figure 10 and 11). It is assumed that bioturbation is inhibited immediately after the impact with a linear increase to undisturbed reference bioturbation intensity within 100 to 200 years.~~

The transient models showed that the impact of the removal of the reactive upper 10 cm layer is much more severe and longer lasting compared to the 'oxygen flooding' scenario. And simulations show no distinguishable difference if 8 or 12 cm are removed instead of 10. This is because the greatest disturbance effect is caused by the absence of the labile organic matter fraction, which is restricted mostly to the upper 10 centimetres of the sediment.

Short term impact. Immediately after the removal of the highly reactive surface sediment, solute profiles are in strong disequilibrium and mostly diffusion controlled. This is especially true for oxygen, which rapidly diffuses into previously anoxic sediments. The Fe(II) layer plays an insignificant role in the initial post-impact weeks but commences to inhibit further penetration of the oxygen front at 5 weeks. In the absence of the reactive surface layer, organic matter degradation rates, which strongly shape the reference oxygen profile, play only a minimal role in the weeks after the disturbance. The modelled 'removal' profiles agree well with the analytical in situ oxygen profiles of the 5 week old EBS track and confirm that the linear nature of the analytical profiles is likely

shaped by a mixture of a downward diffusing oxygen front and the initiation of the oxygen-Fe(II) reaction layer. For comparison, impact simulations assuming full recovery of the bioturbation intensity by 200 years instead of 100 years, are also shown. Here, the oxygen profile is also distinctly more linear but even more reduced sediment mixing through bioturbation allows oxygen to penetrate slightly deeper (18 cm.b.s.f.) compared to the in situ oxygen profiles (13 cm) and to the 100 year bioturbation recovery interval (10 cm.b.s.f, Figure 10).

The 'oxygen flooding' scenario produces a very different oxygen profile. It is shaped mainly by the reaction of the anomalous oxygen with the reactive (labile) organic matter, especially in the upper centimeters where the labile organic matter is most concentrated. The difference to the EBS track in situ profiles supports the observation that the EBS track is mainly affected by sediment removal, rather than mixing (Figure 11).

Medium term impact. The existence of the Fe(II)-oxygen reaction layer plays a particularly important role in the decades after the disturbance. Oxygen is less efficiently removed from the pore water in both scenarios: Removal of the reactive layer significantly reduces oxygen uptake through organic matter degradation and the reactivity of the organic matter was reduced due to reaction with the anomalous flooding with oxygen. In the absence of an oxygen impeding reaction layer, oxygen penetration depths would consequently be significantly increased in both cases (Figure 10 and 11). Simulating the 26 year old DISCOL disturbance has shown that the existence of an oxygen consuming reaction layer is a necessary prerequisite. The 'removal scenario' produces slightly more linear profiles compared to the 'oxygen flooding' simulation because of the relative importance of the Fe(II)-oxygen reaction layer over organic matter degradation process. The slight misfit of both scenarios with the in situ oxygen data suggests that the DEA tracks are most likely affected by a mixture of both scenarios, possible leveled out by lateral diffusion effects. Ongoing organic matter flux at the surface sediment builds up a new post-impact reactive layer with reactivities higher than in the reference model due to the ineffective mixing into deeper sediments through bioturbation (Figure 10 and 11). Thus, differences between bioturbation recovery scenarios, i.e. 100 and 200 years, increase over time with an increasing amount of fresh organic matter that can potentially be mixed into the sediment.

Long term impact. It takes centuries for the geochemical processes to completely recover after the removal of the upper reactive sediment. While the observed geochemical profiles of the disturbed sites show surprisingly little variation compared to the reference site, overall surface fluxes vary significantly during the first 100 years after the impact. This is especially true for the oxygen flux into the sediment, which is more than halved within the first year of the impact (Figure 10). Within the first decades after the impact the build-up of the labile organic matter, and its mixing into deeper sediment through bioturbation, gains influence. With increasing depletion of oxygen through organic matter degradation, oxygen concentrations decrease alongside with Fe(II)-oxygen reaction rates. The transition from Fe(II)-controlled to organic matter-controlled oxygen profiles is accompanied by a slight increase in the oxygen penetration depth (Figure 10). The exact quantification of this transition is difficult to estimate, but the fact that 26 years after the impact oxygen profiles are still efficiently impeded by the Fe(II)-oxygen reaction layer suggests that this process will significantly reduce the oxygen penetration depth until the organic matter degradation rates are near pre-disturbance levels (ca. 100 years after the impact). Interestingly, while steady-state biogeochemical processes strongly depend on the depth and intensity of bioturbation (Haeckel et al., 2001), the time frame of the bioturbation recovery has very little influence on the overall impact recovery process (Figure 10). This is due to the fact, that the limiting factor is

the availability of labile organic matter, which is replenished on a much longer time scale compared to the faunal recovery (Stratmann et al., 2018a).

Recovery of the sediment that was affected by the 'oxygen flooding' scenario is occurring within 100 years and is already in a near pre-impact state 1 year after the disturbance. Here, the Fe(II)-oxygen reaction layer is predominantly responsible for restricting the anomalously high oxygen levels within the upper 20 cm of the sediment. Organic matter degradation rates remain high throughout the recovery process and build-up of fresh labile organic matter that replenishes the loss through the introduction of anomalous oxygen concentration occurs within the recovery phase of the bioturbation (Figure 11).

4. Discussion

The benthic ecosystem is shaped by a balanced interplay of physical, chemical and biological factors, which are fueled by the deposition of organic matter, especially its labile fraction (Figure 12): The degradation of organic matter is microbially catalyzed and in turn provides nutrients to the microbial community (e.g. Witte et al., 2003a; Moodley et al., 2005; Stratmann et al., 2018b; Sweetman et al., 2018). The associated microbial growth provides biomass that sustains meio and macrofauna and forms an important component of the benthic food web (Witte et al., 2003b; Van Oevelen et al., 2006; Van Oevelen et al., 2011). The concomitant bioturbation of the sediment induces a variety of changes, such as lowering the sediment shear strength and the vertical transport of fresh reactive organic matter into deeper sediments (bioturbation) through burrowing invertebrates (Krantzberg, 1985, and references therein). The occurrence of labile organic matter in deeper sediments where oxygen is not as easily replenished compared to surface sediments places an important restriction on the oxygen penetration depth (Haeckel et al., 2001). Bioturbation plays thus a deciding factor in early-diagenetic, especially redox sensitive, processes. These are typically closely linked to the microbial functions and with the introduction of fresh and digested organic matter at depth by infauna new material for additional degradation and microbial colonization, close the causal cycle (Levin et al., 1997; Witte et al., 2003a; Middelburg, 2018). Changes in any compartment of the ecosystem functions will entail modifications of all biogeochemical processes. A natural example is the long-term glacial/interglacial or short-term ENSO driven change in the depositional flux of organic matter to the seafloor imposing gradual cycles in the redox zonation of the sediment (König et al., 2001).

Mining the seafloor will have an abrupt and direct impact on several benthic ecosystem functions at a time: (i) through the removal of all seafloor fauna (Vanreusel et al., 2016; Jones et al., 2017; Gollner et al., 2017; Bluhm, 2001; Borowski, 2001), (ii) through changing the physical characteristics of the sediment surface, i.e. by exposing more compacted sediments with increased shear strength, and removing manganese nodules as hard-substrate habitats (Grupe et al., 2001) and (iii) through the displacement and removal of labile organic matter.

Biological, geochemical and numerical results of the MiningImpact project significantly improve our understanding of the interlinked ecosystem recovery processes in the deep-sea. Removal of the upper reactive surface layer and its fauna will halt bioturbation and organic degradation rates and significantly decrease microbial activity (Figure 12A and B). Based only on deep-sea typical microbial biomass turnover rates and conservative bacterial doubling times, recovery of microbial abundances should occur within 2 – 10 years. Observations show, however, that the microbial activity remained significantly reduced in the decades following the DISCOL disturbance experiment (Vonnahme et al., in press). Microbial recovery thus appears controlled by

Formatted: Highlight

Formatted: Highlight

Formatted: Highlight

Formatted: Highlight

the re-establishment of the labile organic matter fraction, which is still significantly reduced at this times scale. Low nutrient fluxes and the downsized microbial biomass cannot sustain pre-impact faunal abundances (Stratmann et al., 2018a), and recolonization is obstructed by the comparatively hard substrate and absence of hard-substrate habitats (nodule surface) in impacted areas (Vonnahme et al., in press). This directly affects the macrofaunal efficiency to mix surface sediments into deeper layers which is presented in the simulations by the reduced bioturbation coefficient (Figure 12). It should be noted that even if sediment physical conditions and organic matter availability have recovered, it is unclear whether the pre-impact infauna is still available to recolonize the disturbed area.

Prognostic simulations showed that the time scale of the ecosystem recovery ultimately depends only on one factor: the availability of labile organic matter. The amount of reactive organic matter determines the intensity of the food-web activity (i.e. summed carbon cycling, Stratmann et al. (2018a)) and has to reach pre-impact levels to allow for the interlinked ecosystem to recover. In this context, two aspects should be particularly emphasized: (i) deep-sea sediments are characterized by extremely low surface sedimentation rates (~0.004 cm/a) and complete recovery of the labile organic matter fraction takes up to 1000 years (Figure 12). In the Clarion-Clipperton Zone, located also in the abyssal plains of the Pacific Ocean, surface sedimentation rates are even lower (0.0002 – 0.001 cm/a; Volz et al. (2018)). In this area, where nodule mining is expected to commence, potential impact recovery after removal of the upper reactive layer was predicted to occur on an even longer (millennia) time scale (Volz et al., under review). (ii) Ecosystem impact and consequent recovery is strongly dependent on the type of disturbance, more precisely, on the amount of labile organic matter removed. Microbial activity at disturbed sites could be directly correlated to an arbitrary disturbance gradient (Vonnahme et al., in press), which in turn coincides with the thickness of the reactive dark brown surface sediments that was removed during the experimental disturbance. These findings are in line with the results of the prognostic simulations, which showed that the impact is much less severe and recovery times significantly reduced (decades, Figure 11) if sediments are simply mixed or affected by resettling sediment (‘oxygen flooding’ scenario), compared to the removal of the upper reactive layer (centuries, Figure 10 and 12).

5. Conclusions

Previous diagenetic models of the DEA (Haeckel et al., 2001) were updated by a field-based bioturbation coefficient and application of a 3G-organic matter model. A near-surface Fe(II)-oxygen reaction layer was introduced in the prognostic simulations, which represents the refractory Fe(II) phase that did not react with the downward progressing interglacial nitrate front. The surprisingly similar oxygen penetration depths in reference and 26 year old disturbed sediments indicates that this refractory Fe(II) appears to be an efficient barrier for the progressing oxygen front thus defying previous impact simulation that predicted a significant downward migration of the oxygen front (König et al., 2001).

Transient simulation results have significantly enhanced the quality of the interpretation of the observed geochemical profiles, which on first sight do not exhibit marked differences among the various disturbed and reference sites. The geochemical recovery after a mining related removal of the upper reactive sediment layer can be divided into three stages: (i) the initial diffusion driven equilibration of the post-impact profiles (within weeks of the impact), (ii) burn down of the Fe(II)-oxygen reaction layer (decades after the impact) and (iii) re-establishment of the reactive organic matter layer (centuries after the impact). If the reactive surface sediment is

not removed but instead mixed or temporarily re-suspended, anomalously high oxygen concentrations alter biogeochemical processes on a decadal scale, albeit much less severe.

The interdisciplinary (geochemical, numerical and biological) approach to characterise the impact of benthic disturbances on early diagenetic processes provided valuable information on post-impact processes. On one hand it identifies variables that are suitable as indicators of benthic ecosystem health and also allow identification of significant adverse change of the benthic environment. Metabolites of microbial activity were found to be particularly sensitive to disturbances and can even resolve grades of impact (Vonnahme et al., in press). Biogeochemical processes responded more subtle to the disturbance with oxygen, nitrite and bioturbation activity being the most suitable variables. On the other hand, this work highlights the closely linked nature of different benthic ecosystem functions, which is also true during the recovery from mining impacts. The main factor constraining the time frame of the geochemical recovery is the availability of reactive (labile) organic matter, emphasizing the importance of the impact type (sediment removal versus mixing and resuspension) and also the natural depositional flux of organic matter onto the sediment surface (e.g. DEA versus the Clarion-Clipperton Zone). The microbial degradation of the available reactive organic matter fraction defines the base of the food web structure, which eventually sustains metazoans. Some of the epifauna burrows into the seafloor (bioturbation) and in turn has a critical influence on geochemical, especially redox sensitive, processes and fluxes. Recovery of the system is thus only possible if the ecosystem functions of all compartments are restored. Our results also show that it is important to identify regional specialties, such as the reactive Fe(II) layer in DISCOL sediments, because they may affect the biogeochemical response to a benthic disturbance drastically.

While biogeochemical fluxes may recover close to the pre-impact state, the nodule ecosystem cannot recover, since the essential hard substrate, the polymetallic nodules, have been removed. Consequently, a new nodule-free ecosystem with very different faunal communities, functions and services has to establish in the mining areas and its thickly blanketed surrounding. Furthermore, this new ecosystem will take much longer time scales to establish because it is largely controlled by the recovery of the underlying biogeochemical fluxes and processes that fuel abyssal life.

Acknowledgements

The authors would like to thank A. Bleyer, R. Surberg, B. Domeyer and K. Hamann for co-working on sample collection on RV Sonne and onboard and onshore pore water analyses. P. van Gaever is thanked for carrying out the radionuclide analysis. We are also indebted to the captain and crew of RV SONNE for their invaluable support during the cruise SO242. We are grateful for the constructive comments of two anonymous reviewers. This work was funded by the German Federal Ministry of Education and Research through the MiningImpact project (grant no. 03F0707A, 03F0707D, 03F0812A and 03F0812D) of the Joint Programming Initiative of Healthy and Productive Seas and Oceans (JPIO). The authors are solely responsible for the content of this paper.

Data availability

The geochemical data presented in Figure 3, 4 and ~~5~~ 6 are publically available in the PANGAEA database with the DOI https://doi.org/10.1594/PANGAEA.905377. The PANGAEA database also hosts the activity measurements of the ^{210}Pb series presented Figure 7 with the DOIs https://doi.org/10.1594/PANGAEA.905442 (alpha spectrometry) and https://doi.org/10.1594/PANGAEA.905443 (gamma spectrometry).

References

Berner, R. A.: Early Diagenesis - A Theoretical Approach, Princeton University Press, Princeton, New Jersey, 241 pp., 1980.

Bluhm, H.: Re-establishment of an abyssal megabenthic community after experimental physical disturbance of the seafloor, Deep-Sea Research Part Ii-Topical Studies in Oceanography, 48, 3841-3868, Doi 10.1016/S0967-0645(01)00070-4, 2001.

Boetius, A.: RV SONNE Cruise Report SO242-2: JPI OCEANS Ecological Aspects of Deep-Sea Mining, DISCOL Revisited, 2015.

Borowski, C., and Thiel, H.: Deep-sea macrofaunal impacts of a large-scale physical disturbance experiment in the Southeast Pacific, Deep Sea Research Part II: Topical Studies in Oceanography, 45, 55-81, 10.1016/S0967-0645(97)00073-8, 1998.

Borowski, C.: Physically disturbed deep-sea macrofauna in the Peru Basin, southeast Pacific, revisited 7 years after the experimental impact, Deep-Sea Research II, 48, 3809-3839, 2001.

Boudreau, B. P.: Diagenetic Models and Their Implementation: Modelling Transport and Reactions in Aquatic Sediments, Springer-Verlag, Berlin, Heidelberg, New York, 414 pp., 1996.

Breland, J., and Byrne, R.: Spectrophotometric procedures for determination of sea water alkalinity using bromcresol green, Deep-Sea Research I, 40, 629-641, 1993.

Brenke, N.: An Epibenthic sledge for operations on marine soft bottom and bedrock, Marine Technology Society Journal, 39, 10-21, Doi 10.4031/002533205787444015, 2005.

Drodt, M., Trautwein, A. X., König, I., Suess, E., and Koch, C. B.: Mössbauer spectroscopic studies on the iron forms of deep-sea sediments, Physics and Chemistry of Minerals, 24, 281-293, 10.1007/s002690050040, 1997.

Froelich, P. N., Klinkhammer, G. P., Bender, M. L., Luedtke, N. A., Heath, G. R., Cullen, D., Dauphin, P., Hammond, D., Hartman, B., and Maynard, V.: Early oxidation of organic matter in pelagic sediments of the eastern equatorial Atlantic: suboxic diagenesis, Geochimica et Cosmochimica Acta, 43, 1075-1090, 1979.

Gollner, S., Kaiser, S., Menzel, L., Jones, D. O. B., Brown, A., Mestre, N. C., van Oevelen, D., Menot, L., Colaco, A., Canals, M., Cuvelier, D., Durden, J. M., Gebruk, A., Egho, G. A., Haeckel, M., Marcon, Y., Mevenkamp, L., Morato, T., Pham, C. K., Purser, A., Sanchez-Vidal, A., Vanreusel, A., Vink, A., and Martinez Arbizu, P.: Resilience of benthic deep-sea fauna to mining activities, Mar Environ Res, 129, 76-101, 10.1016/j.marenvres.2017.04.010, 2017.

Goloway, F., and Bender, M.: Diagenetic models of interstitial nitrate profiles in deep sea suboxic sediments, Limnology and Oceanography, 27, 624-638, 1982.

Grasshoff, K., Ehrhardt, M., and Kremling, K.: Methods of Seawater Analysis, 3 ed., Wiley-VCH, Weinheim, 600 pp. pp., 1999.

Greinert, J.: RV SONNE Cruise Report SO242-1 JPI OCEANS Ecological Aspects of Deep-Sea Mining DISCOL Revisited, GEOMAR, 2015.

Grupe, B., Becker, H. J., and Oebius, H. U.: Geotechnical and sedimentological investigations of deep-sea sediments from a manganese nodule field of the Peru Basin, Deep Sea Research Part II: Topical Studies in Oceanography, 48, 3593-3608, 10.1016/s0967-0645(01)00058-3, 2001.

Haeckel, M., König, I., Riech, V., Weber, M., and Suess, E.: Pore water profiles and numerical modelling of Peru Basin deep-sea sediments, Deep-Sea Research II, 48, 3713-3736, 2001.

Hessler, R. R., and Jumars, P. A.: Abyssal community analysis from replicate box cores in the central North Pacific, Deep-Sea Research I, 21, 185-209, 1974.

Jahnke, R. A., Emerson, S. R., Reimers, C. E., Schuffert, J., Ruttenberg, K., and Archer, D.: Benthic recycling of biogenic debris in the eastern tropical Atlantic Ocean, Geochimica et Cosmochimica Acta, 53, 2947-2960, 1989.

Jones, D. O., Kaiser, S., Sweetman, A. K., Smith, C. R., Menot, L., Vink, A., Trueblood, D., Greinert, J., Billett, D. S., Arbizu, P. M., Radziejewska, T., Singh, R., Ingole, B., Stratmann, T., Simon-Lledo, E., Durden, J. M., and Clark, M. R.: Biological responses to disturbance from simulated deep-sea polymetallic nodule mining, PLoS One, 12, e0171750, 10.1371/journal.pone.0171750, 2017.

Jorgensen, B. B.: A comparison of methods for the quantification of bacterial sulfate reduction in coastal marine sediments. II. Calculation from mathematical models, Geomicrobiology Journal, 1, 29-47, 10.1080/01490457809377722, 1978.

König, I., Drodt, M., Suess, E., and Trautwein, A. X.: Iron reduction through the tan-green color transition in deep-sea sediments, Geochimica et Cosmochimica Acta, 61, 1679-1683, 1997.

Formatted: Left, Indent: Left: 0", Hanging: 0.5"

König, I., Haeckel, M., Drodt, M., Suess, E., and Trautwein, A. X.: Reactive Fe(II) layers in deep-sea sediments, Geochimica et Cosmochimica Acta, 63, 1517-1526, 1999.
König, I., Haeckel, M., Lougear, A., Suess, E., and Trautwein, A. X.: A geochemical model of the Peru Basin deep-sea floor and the response of the system to technical impacts, Deep-Sea Research II, 48, 3737-3756, 2001.
Krantzberg, G.: The Influence of Bioturbation on Physical, Chemical and Biological Parameters in Aquatic Environments: A Review Environmental Pollution (Series A), 39, 99-122, 1985.
Levin, L., Blair, N., DeMaster, D., Plaia, G., Fornes, W., Martin, C., and Thomas, C.: Rapid subduction of organic matter by maldanid polychaetes on the North Carolina slope, Journal of Marine Research, 55, 595-611, 1997.
Luff, R., and Wallmann, K.: Fluid flow, methane fluxes, carbonate precipitation and biogeochemical turnover in gas hydrate-bearing sediments at Hydrate Ridge, Cascadia Margin: Numerical modeling and mass balances, Geochimica et Cosmochimica Acta, 67, 3403-3421, 2003.
Lyle, M.: The brown-green color transition in marine sediments: A marker of the Fe(III)-Fe(II) redox boundary, Limnology and Oceanography, 28, 1026-1033, 1983.
Martin, W. R., Bender, M., Leinen, M., and Orchardo, J.: Benthic organic carbon degradation and biogenic silica dissolution in the central equatorial Pacific, Deep-Sea Research, 38, 1481-1516, 1991.
Middelburg, J. J.: A simple rate model for organic-matter decomposition in marine-sediments, Geochimica et Cosmochimica Acta, 53, 1577-1581, 1989.
Middelburg, J. J.: Reviews and syntheses: to the bottom of carbon processing at the seafloor, Biogeosciences, 15, 413-427, 10.5194/bg-15-413-2018, 2018.
Moodley, L., Middelburg, J. J., Soetaert, K., Boschker, H. T. S., Herman, P. M. J., and Heip, C. H. R.: Similar rapid response to phytodetritus deposition in shallow and deep-sea sediments, Journal of Marine Research, 63, 457-469, 2005.
Murray, J. W., Grundmanis, V., and Smethie, W. M.: Interstitial water chemistry in the sediments of Saanich Inlet, Geochimica et Cosmochimica Acta, 42, 1011-1026, 1978.
Paul, S. A. L., Gaye, B., Haeckel, M., Kasten, S., and Koschinsky, A.: Biogeochemical Regeneration of a Nodule Mining Disturbance Site: Trace Metals, DOC and Amino Acids in Deep-Sea Sediments and Pore Waters, Frontiers in Marine Science, 5, 10.3389/fmars.2018.00117, 2018.
Paul, S. A. L., Haeckel, M., Bau, M., Bajracharya, R., and Koschinsky, A.: Small-scale heterogeneity of trace metals including rare earth elements and yttrium in deep-sea sediments and porewaters of the Peru Basin, southeastern equatorial Pacific, Biogeosciences, 16, 4829-4849, 10.5194/bg-16-4829-2019, 2019.
Rabouille, C., and Gaillard, J.-F.: Towards the EDGE: Early diagenetic global explanation. A model depicting the early diagenesis of organic matter, O_2, NO_3, Mn, and PO_4, Geochimica et Cosmochimica Acta, 55, 2511-2525, 1991a.
Rabouille, C., and Gaillard, J.-F.: A coupled model representing the deep-sea organic carbon mineralization and oxygen consumption of surficial sediments, Journal of Geophysical Research, 96, 2761-2776, 1991b.
Schriever, G., and Thiel, H.: Cruise Report DISCOL 3, Sonne cruise 7, Universität Hamburg, 59, 1992.
Stratmann, T., Lins, L., Purser, A., Marcon, Y., Rodrigues, C. F., Ravara, A., Cunha, M. R., Simon-Lledó, E., Jones, D. O. B., Sweetman, A. K., Köser, K., and van Oevelen, D.: Abyssal plain faunal carbon flows remain depressed 26 years after a simulated deep-sea mining disturbance, Biogeosciences, 15, 4131-4145, 10.5194/bg-15-4131-2018, 2018a.
Stratmann, T., Mevenkamp, L., Sweetman, A. K., Vanreusel, A., and van Oevelen, D.: Has Phytodetritus Processing by an Abyssal Soft-Sediment Community Recovered 26 Years after an Experimental Disturbance?, Frontiers in Marine Science, 5, 10.3389/fmars.2018.00059, 2018b.
Sweetman, A. K., Smith, C. R., Shulse, C. N., Maillot, B., Lindh, M., Church, M. J., Meyer, K. S., Oevelen, D., Stratmann, T., and Gooday, A. J.: Key role of bacteria in the short-term cycling of carbon at the abyssal seafloor in a low particulate organic carbon flux region of the eastern Pacific Ocean, Limnology and Oceanography, 64, 694-713, 10.1002/lno.11069, 2018.
Thiel, H., and Schriever, G.: Deep-sea mining, environmental impact and the DISCOL project, Ambio, 19, 245-250, 1990.
Van Oevelen, D., Moodley, L., Soetaert, K., and Middelburg, J. J.: The trophic significance of bacterial carbon in a marine intertidal sediment: Results of an in situ stable isotope labeling study, Limnology and Oceanography, 51, 2349-2359, 2006.
Van Oevelen, D., Bergmann, M., Soetaert, K., Bauerfeind, E., Hasemann, C., Klages, M., Schewe, I., Soltwedel, T., and Budaeva, N. E.: Carbon flows in the benthic food web at the deep-sea observatory HAUSGARTEN (Fram Strait), Deep-Sea Research I, 58, 1069-1083, 2011.
Vanreusel, A., Hilario, A., Ribeiro, P. A., Menot, L., and Arbizu, P. M.: Threatened by mining, polymetallic nodules are required to preserve abyssal epifauna, Sci Rep, 6, 26808, 10.1038/srep26808, 2016.

Volz, J. B., Mogollon, J. L., Geibert, W., Arbizu, P. M., Koschinsky, A., and Kasten, S.: Natural spatial variability of depositional conditions, biogeochemical processes and element fluxes in sediments of the eastern Clarion-Clipperton Zone, Pacific Ocean, Deep-Sea Research Part I, 140, 159-172, 2018.

Volz, J. B., L., H., Haeckel , M., Koschinsky, A., and Kasten, S.: Impact of small-scale disturbances on geochemical conditions, biogeochemical processes and element fluxes in surface sediments of the eastern Clarion-Clipperton Zone, Pacific Ocean, Biogeosciences, under review.

Vonnahme, T. R., Molari, M., Janssen, F., Wenzhöfer, F., Haeckel, M., Titschack, J., and Boetius, A.: Effects of a deep-sea mining experiment on seafloor microbial communities and functions after 26 years, Science Advances, in press.

Weber, M. E., von Stackelberg, U., Marchig, V., Wiedicke, M., and Grupe, B.: Variability of surface sediments in the Peru basin: dependence on water depth, productivity, bottom water flow, and seafloor topography, Marine Geology, 163, 169-184, 10.1016/s0025-3227(99)00103-6, 2000.

Welicky, K., Suess, E., Ungerer, C. A., Müller, P. J., and Fischer, K.: Problems with accurate carbon measurements in marine sediments and particulate matter in seawater: A new approach, Limnology and Oceanography, 28, 1252-1259, 1983.

Westrich, J. T., and Berner, R. A.: The role of sedimentary organic matter in bacterial sulfate reduction: The G model tested, Limnology and Oceanography, 29, 236-249, 1984.

Wilson, T. R. S., Thomson, J., Colley, S., Hydes, D. J., Higgs, N. C., and Sørensen, J.: Early organic diagenesis: The significance of progressive subsurface oxidation fronts in pelagic sediments, Geochimica et Cosmochimica Acta, 49, 811-822, 1985.

Witte, U., Aberle, N., Sand, M., and Wenzhöfer, F.: Rapid response of a deep-sea benthic community to POM enrichment: an in situ experimental study, Marine Ecology Progress Series, 251, 27-36, 2003a.

Witte, U., Wenzhöfer, F., Sommer, S., Boetius, A., Heinz, P., Aberle, N., Sand, M., Cremer, A., Abraham, W.-R., Jørgensen, B. B., and Pfannkuche, O.: In situ experimental evidence of the fate of a phytodetritus pulse at the abyssal sea floor, Nature, 424, 763-766, 2003b.

Formatted: Indent: Left: 0", Hanging: 0.5"

Formatted: Indent: Left: 0.06", Hanging: 0.5"

Formatted: Left, Indent: Left: 0.06", Hanging: 0.5"

Tables

Table 1. Sampling station locations and description

Area	Station	Description	Latitude (S)	Longitude (W)	Water Depth / m
Reconnaissance					
Outside DEA					
		Southern reference			
	38 GC 1	southern reference with nodules	7°07.537'	88°27.047'	4161
	34 MUC 6	southern reference with nodules	7°07.524'	88°27.031'	4162
		Western reference			
	89 GC 4	western reference with nodules	7°04.562'	88°31.577'	4125
	80 MUC 22	western reference with nodules	7°04.542'	88°31.581'	4130
		Eastern reference			
	123 GC 6	eastern reference with(out) nodules	7°06.045'	88°24.848'	4208
	119 MUC 31	eastern reference with(out) nodules	7°06.033'	88°24.826'	4204
		Volcano crater			
	132 GC 7	small volcano crater with dense nodules	7°03.369'	88°26.031'	4152
	129 BC 26	small volcano crater with dense nodules	7°03.373'	88°26.026'	4144
Inside DEA					
		DEA plough tracks			
	51 GC 2	DEA west plough tracks	7°04.411'	88°27.836'	4148
	56 MUC 12	DEA west plough tracks	7°04.414'	88°27.760'	4149
	61 MUC 13	DEA west outside plough tracks	7°04.378'	88°27.781'	4148
	70 MUC 17	DEA west resettled sediment plume	7°04.400'	88°27.778'	4128
		DEA black patch			
	84 GC 3	DEA black patch in sidescan sonar	7°03.951'	88°27.093'	4146
	74 MUC 20	DEA black patch in sidescan sonar	7°03.945'	88°27.097'	4150
		DEA central/trough			
	100 GC 5	DEA central	7°04.342'	88°27.442'	4151
	108 MUC 26	DEA central	7°04.483'	88°26.919'	4169
Microhabitats					
		Reference			
	34 MUC 6	southern reference with nodules	7°07.524'	88°27.031'	4162
	80 MUC 22	western reference with nodules	7°04.542'	88°31.581'	4130
	119 MUC 31	eastern reference with(out) nodules	7°06.033'	88°24.826'	4204
		DEA outside tracks			
	61 MUC 13	DEA west outside plough track	7°04.378'	88°27.781'	4148
	146 ROV PC79	DEA west 20 m off plough track	7°04.4000'	88°27.8266'	4140
	166 ROV PC70	DEA east 20 m off plough track	7°04.4585'	88°26.9240'	4143
	229 MUC	DEA south outside plough track	7°04.6970'	88°27.3970'	4133
		DEA track furrow			
	146 ROV PC77	DEA west plough furrow	7°04.4110'	88°27.8363'	4139
	166 ROV PC69	DEA east plough furrow	7°04.4780'	88°26.9178'	4143
	219 ROV PC75	DEA south plough furrow	7°04.6930'	88°27.4540'	4155
		DEA ridge			

Formatted ... (repeated)

142 ROV PC33	DEA west plough ridge	7°04.4094'	88°27.8330'	4139
163 ROV PC83	DEA east plough ridge	7°04.4926'	88°26.9333'	4143
232 ROV PC64	DEA south plough ridge	7°04.6890'	88°27.4554'	4156
	DEA subsurface patch			
142 ROV PC48	DEA west subsurface patch	7°04.4113'	88°27.8127'	4140
169 ROV PC83	DEA east subsurface patch	7°04.4808'	88°26.9130'	4144
219 ROV PC58	DEA south subsurface patch	7°04.6930'	88°27.4540'	4155
	EBS track			
202 ROV PC80	DEA west inside EBS track	7°04.9533'	88°28.1980'	4150
202 ROV PC18	DEA west side pile EBS track	7°04.9609'	88°28.1907'	4150
211 ROV PC52	DEA west rim inside EBS track	7°04.9581'	88°28.1909'	4150
211 ROV PC73	DEA west outside of EBS track	7°04.9669'	88°28.1929'	4150
In situ oxygen profiles				
	Reference			
158 LANDER-#1	Reference South	7°7.4590'	88°26.9740'	4155
	Undisturbed DEA			
176 ROV profiler #1	DEA E outside track	7°4.4677'	88°26.9187'	4102
169 ROV profiler #1	DEA E outside track	7° 4.4563'	88°26.9176'	4102
213 ROV profiler #2	EBS outside track	7°5.0220'	88°28.1526'	4189
146 ROV profiler #2	DEA W outside track	7°4.4000'	88°27.8274'	4140
	DEA plough tracks			
176 ROV profiler #2	Subsurface	7°4.4762'	88°26.9190'	4102
154 ROV profiler #2	Subsurface	7°4.4118'	88°27.8172'	4101
166 ROV profiler #2	Furrow	7°4.4898'	88°26.9286'	4104
169 ROV profiler #2	Furrow	7°4.4787'	88°26.9205'	4104
	EBS track			
202 ROV profiler #1	Inside track	7°4.9787'	88°28.1730'	4189

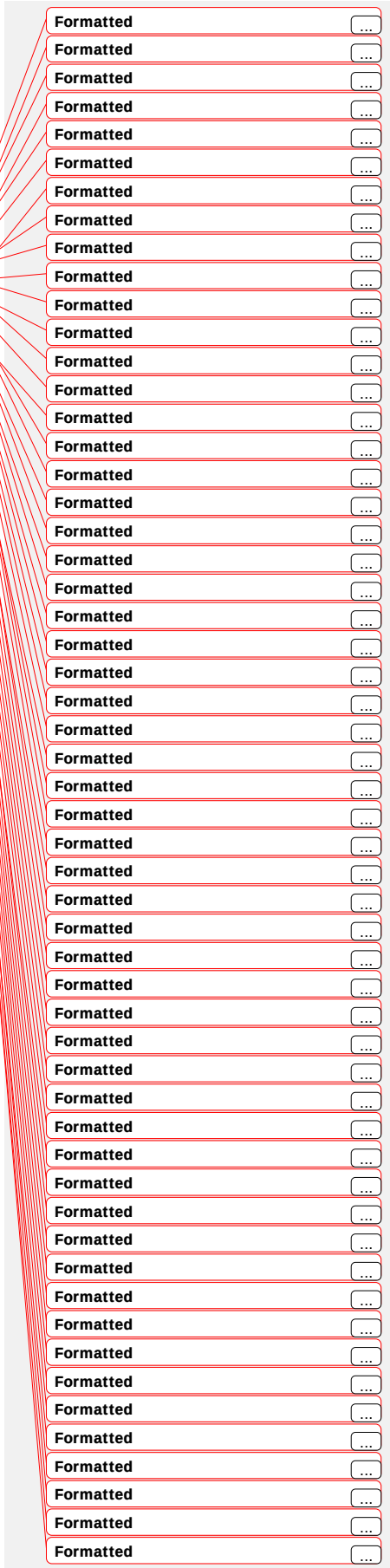

Table 2. Summary of analysed properties, analytical methods, estimated analytical errors, and detection limits

Parameter	Method	Error (detection limit)[a]
NO_3^-	Spectrophotometer (as sulphanile-a-naphthylamide)[b]	(1 µmol l^{-1})
NO_2^-	Spectrophotometer (as sulphanile-a-naphthylamide)[b]	(1 µmol l^{-1})
NH_4^+	Spectrophotometer (as indophenol blue)b	(1 µmol l^{-1})
Mn^{2+}	ICP-AES	5-10% (1 µmol l^{-1})
SO_4^{2-}	Ion chromatography	0.8-1.2 mmol l^{-1} (5 mmol l^{-1})
C_{org}	CHN-Analyser[c]	0.04 wt%
Alkalinity	Titration[d]	0.05 meq l^{-1}
Porosity	Weight difference before and after drying of the sediment	0.02

[a] Note. For some properties no analytical error could be determined because of few data points or concentrations close to the detection limit.

[b] Grasshoff et al. (1999).

[c] Welicky et al. (1983).

[d] Breland and Byrne (1993).

Formatted: Left, Indent: Left: 0.06", Hanging: 0.5"

Formatted: Left, Indent: Left: 0.06", Hanging: 0.5"

Formatted: Left, Indent: Left: 0.06", Hanging: 0.5"

Formatted: Left, Indent: Left: 0.06", Hanging: 0.5"

Formatted: Left, Indent: Left: 0.06", Hanging: 0.5"

Formatted: Left, Indent: Left: 0.06", Hanging: 0.5"

Formatted: Left, Indent: Left: 0.06", Hanging: 0.5"

Formatted: Left, Indent: Left: 0.06", Hanging: 0.5"

Formatted: Left, Indent: Left: 0.06", Hanging: 0.5"

Formatted: Left, Indent: Left: 0.06", Hanging: 0.5"

Formatted: Left, Indent: Left: 0.06", Hanging: 0.5"

Formatted: Left, Indent: Left: 0.06", Hanging: 0.5"

Formatted: Left, Indent: Left: 0.06", Hanging: 0.5"

Formatted: Left, Indent: Left: 0.06", Hanging: 0.5"

Table 3. Reaction stoichiometry and rate expressions of the organic mater ($(CH_2O)_a(NH_3)_b(H_3PO_4)_c$) degradation and secondary redox reactions. All solute species are in concentrations of $\frac{mmol}{L_{pw}}$ and all solid species in $\frac{mmol}{L_{ds}}$. All reaction rate expressions are stated in the units of $\frac{mmol}{L_{pw}\,a}$ via conversion with $F_{pw} = \left(\frac{1-\phi}{\phi}\right)$.

ID	*Reaction*	*Rate expression (mmol/Lpw/a)*
Organic matter degradation		
	$(CH_2O)_a(NH_3)_b(H_3PO_4)_c + (a+2b)O_2 + (b+2c)HCO_3^- \rightarrow (a+b+2c)\,CO_2 + (b)NO_3^- + (c)HPO_4^{2-} + (a+2b+2c)H_2O$	$\sum_{i=1,2,3} k_i \frac{Corg_i}{a} R_{O2}\,F_{pw}$
	$(CH_2O)_a(NH_3)_b(H_3PO_4)_c + \left(\frac{4}{5}a + \frac{3}{5}b\right)NO_3^- \rightarrow \frac{1}{2}\left(\frac{4}{5}a + \frac{3}{5}b + b\right)N_2 + cHPO_4^{2-} + \left(\frac{3}{5}a + \frac{6}{5}b + 2c\right)H_2O + \left(\frac{1}{5}a - \frac{3}{5}b + 2c\right)CO_2 + \left(\frac{4}{5}a + \frac{3}{5}b - 2c\right)HCO_3^-$	$\sum_{i=1,2,3} k_i \frac{Corg_i}{a} R_{NO3}\,F_{pw}$
	$(CH_2O)_a(NH_3)_b(H_3PO_4)_c + 2a\,MnO_2 + (3a+b-2c)CO_2 + (a+b-2c)H_2O \rightarrow (4a+b-2c)HCO_3^- + 2a\,Mn^{2+} + bNH_4^+ + cHPO_4^{2-}$	$\sum_{i=1,2,3} k_i \frac{Corg_i}{a} R_{MnO2}\,F_{pw}$
Secondary redox reactions		
	$NH_4^+ + 2O_2 + 2HCO_3^- \rightarrow NO_3^- + 2CO_2 + 3H_2O$	$k_{NH4Ox}\,NH_4\,O_2$
	$2Mn^{2+} + O_2 + 4HCO_3^- \rightarrow 2MnO_2 + 4CO_2 + 2H_2O$	$k_{MnOx}\,Mn^{2+}\,O_2$
	$4Fe(II) + O_2 + 2H_2O + 4CO_2 \rightarrow 4Fe(III) + 4HCO_3^-$	$k_{Fe(II)Ox}\,Fe^{2+}\,O_2$
Monod expressions		
	$R_{O2} = \frac{O_2}{K_{O2} + O_2}$	
	$R_{NO3} = \frac{NO_3}{K_{NO3} + NO_3}\;\frac{K_{o2}}{K_{O2} + O_2}$	
	$R_{MnO2} = \frac{MnO_2}{K_{Mn} + MnO_2}\;\frac{K_{NO3}}{K_{NO3} + NO_3}\;\frac{K_{o2}}{K_{O2} + O_2}$	

Formatted: Indent: Left: 0.06", Hanging: 0.5"

Formatted: Left, Indent: Left: 0.06", Hanging: 0.5"

Formatted: Left, Indent: Left: 0.06", Hanging: 0.5"

Formatted: Left, Indent: Left: 0.06", Hanging: 0.5"

Formatted: Left, Indent: Left: 0.06", Hanging: 0.5"

Formatted: Left, Indent: Left: 0.06", Hanging: 0.5"

Formatted: Left, Indent: Left: 0.06", Hanging: 0.5"

Formatted: Left, Indent: Left: 0.06", Hanging: 0.5"

Formatted: Left, Indent: Left: 0.06", Hanging: 0.5"

Formatted: Left, Indent: Left: 0.06", Hanging: 0.5"

Formatted: Left, Indent: Left: 0.06", Hanging: 0.5"

Formatted: Left, Indent: Left: 0.06", Hanging: 0.5"

Formatted: Left, Indent: Left: 0.06", Hanging: 0.5"

Formatted: Left, Indent: Left: 0.06", Hanging: 0.5"

Formatted: Left, Indent: Left: 0.06", Hanging: 0.5"

Formatted: Indent: Left: 0.06", Hanging: 0.5"

Table 4. Constrained and fitted parameters used in the numerical simulations

Parameter	Value	Units	Reference
General parameter			
Temperature	4	°C	a)
Pressure	400	bar	a)
Salinity	35	‰	a)
Redflied ratio (C:N:P)	106:16:01		
Sedimentation rate	0.0004	cm a^{-1}	Haeckel et al. (2001)
Maximu depth of calculation	200	cm	
Number of points in the numerical grid (uneven)	500		
Fitted parameters - background (reference) model			
Porosity at sediment surface (φ_0)	0.94		c)
Porosity at infinite depth (φ_∞)	0.86		c)
Porosity attenuation coefficient (β)	0.14		c)
Bioturbation coefficient (D_b^0)	0.65	cm^2 a^{-1}	b)
Bioturbation half depth (x_{Db})	10	cm	b)
Bioturbation decrease (β_{Db})	4		b)
Flux of labile C_{org} (F_{G0})	10	µmol cm^{-2} a^{-1}	c)
Flux of semi-labile C_{org} (F_{G1})	1.2	µmol cm^{-2} a^{-1}	c)
Flux of refractory C_{org} (F_{G2})	0.06	µmol cm^{-2} a^{-1}	c)
Rate constant for labile C_{org} oxidation (k_{G0})	0.1	a^{-1}	c)
Rate constant for semi-labile C_{org} oxidation (k_{G1})	0.003	a^{-1}	c)
Rate constant for refractory C_{org} oxidation (k_{G2})	5E-07	a^{-1}	c)
~~Rate constant for reaction of Mn^{2+} and NO_3^-~~	~~0.2~~	~~l $mmol^{-1}$ a^{-1}~~	~~c)~~
Rate constant for reaction of Mn^{2+} and O_2	1E+06	l $mmol^{-1}$ a^{-1}	c)
Rate constant for reaction of NH_4^+ and O_2	500	l $mmol^{-1}$ a^{-1}	c)
Monod constant for O_2 reduction	8E-06	mmol	c)
Monod constant for NO_3^- reduction	0.03	mmol	Boudreau (1996)
Monod constant for MnO_2 reduction	10	mmol	Boudreau (1996)
~~Monod constant for SO_4^{2-} reduction~~	~~1~~	~~mmol~~	~~Boudreau (1996)~~
$[MnO_2]_{model\ domain}$	1.9	wt%	a)
$[O_2]_{bottom\ water}$	0.132	mmol l^{-1}	a)
$[NO_3^-]_{bottom\ water}$	0.042	mmol l^{-1}	a)
$[NH_4^+]_{bottom\ water}$	0	mmol l^{-1}	a)
$[Mn^{2+}]_{bottom\ water}$	0	mmol l^{-1}	a)
$[Alkallinity]_{bottom\ water}$	2.4	meq l^{-1}	a)
$[Mn^{2+}]_{lower\ boundary}$	0.05	mmol l^{-1}	a)
Parameter for impact simulations			
Bioturbation recovery time (tD_B)	100 / 200	a	d)
Case 'reactive Fe(II)-O2 layer'			
[Fe(II)] at lower boundary	0.44	wt%	e)
Fe(II) half depth of increase	20	cm	
Fe(II) profile reduction coefficient	2		
Rate constant for reaction of Fe(II) and O_2	100	l $mmol^{-1}$ a^{-1}	c)
Case 'removal'			
Removed sediment thickness	10	cm	d)
Case 'O2 flooding'			

Formatted Table

Formatted Table

$[O2]_{reactive\ layer}$	$= [O_2]_{bottom\ water}$	mmol l^{-1}	
Half depth O_2 decrease	12	cm	
O_2 attenuation coefficient	2.5		
Bioturbation model			
^{210}Pb radioactive decay constant	ln(2)/22.3	a^{-1}	
^{226}RaTh radioactive decay constant	ln(2)/1602	a^{-1}	
^{230}Th radioactive decay constant	ln(2)/57380	a^{-1}	
$[^{210}Pb]_{bottom\ water}$	1.0	Bq g^{-1}	b)
$[^{226}Ra]_{bottom\ water}$	0.3	Bq g^{-1}	b)
$[^{230}Th]_{bottom\ water}$	0.6	Bq g^{-1}	b)

a) Approximated by field data; b) fitted to Pb data (Figure 7); c) fitted to field data; d) Approximated from data and references presented in Volz et al. (submitted); e) Inferred from data presented in König et al. (1997, 1999)

735 **Figures**

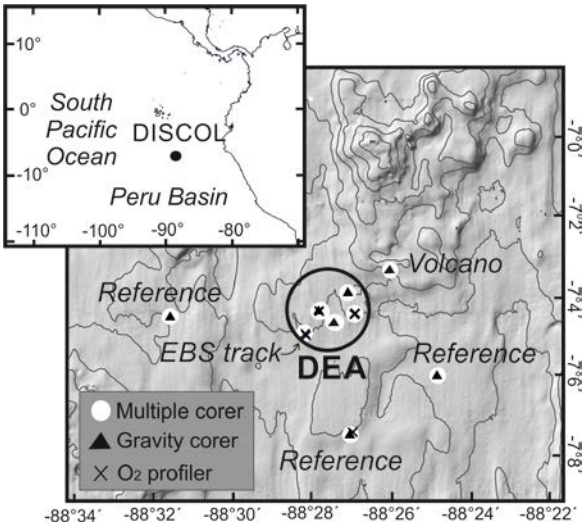

Figure 1. Bathymetric map of the DEA region in the Peru basin including the sampling stations presented in this work. More details on the sampling locations are provided in Table 1.

740

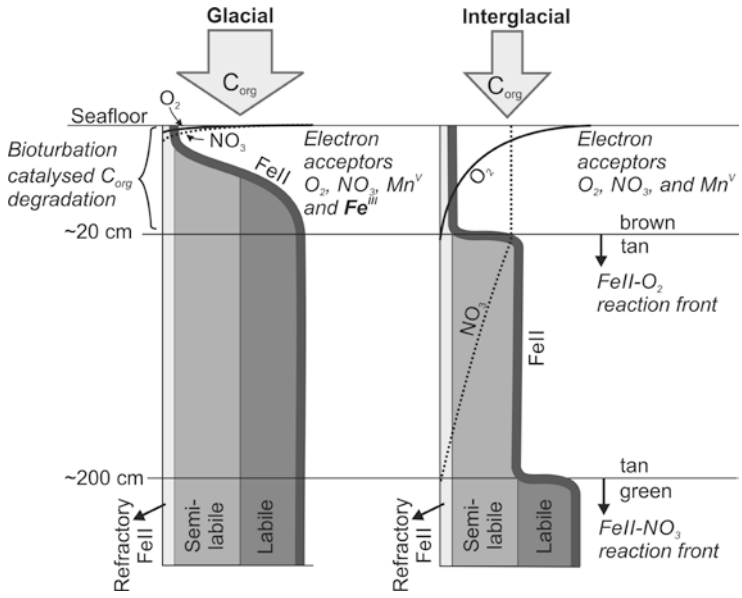

Figure 2. Schematic diagram (not to scale) outlining the formation of a Fe(II) rich clay phase (green) in the context of glacially high organic matter input and its conversion to Fe(III) by downward progressing NO_3 fronts during interglacial periods triggered by reduced organic matter input as postulated by König et al. (2001). In this study, we propose that a second reaction front exists impeding the downward O_2 migration through a reaction with the semi-labile Fe(II) phase.

745

750

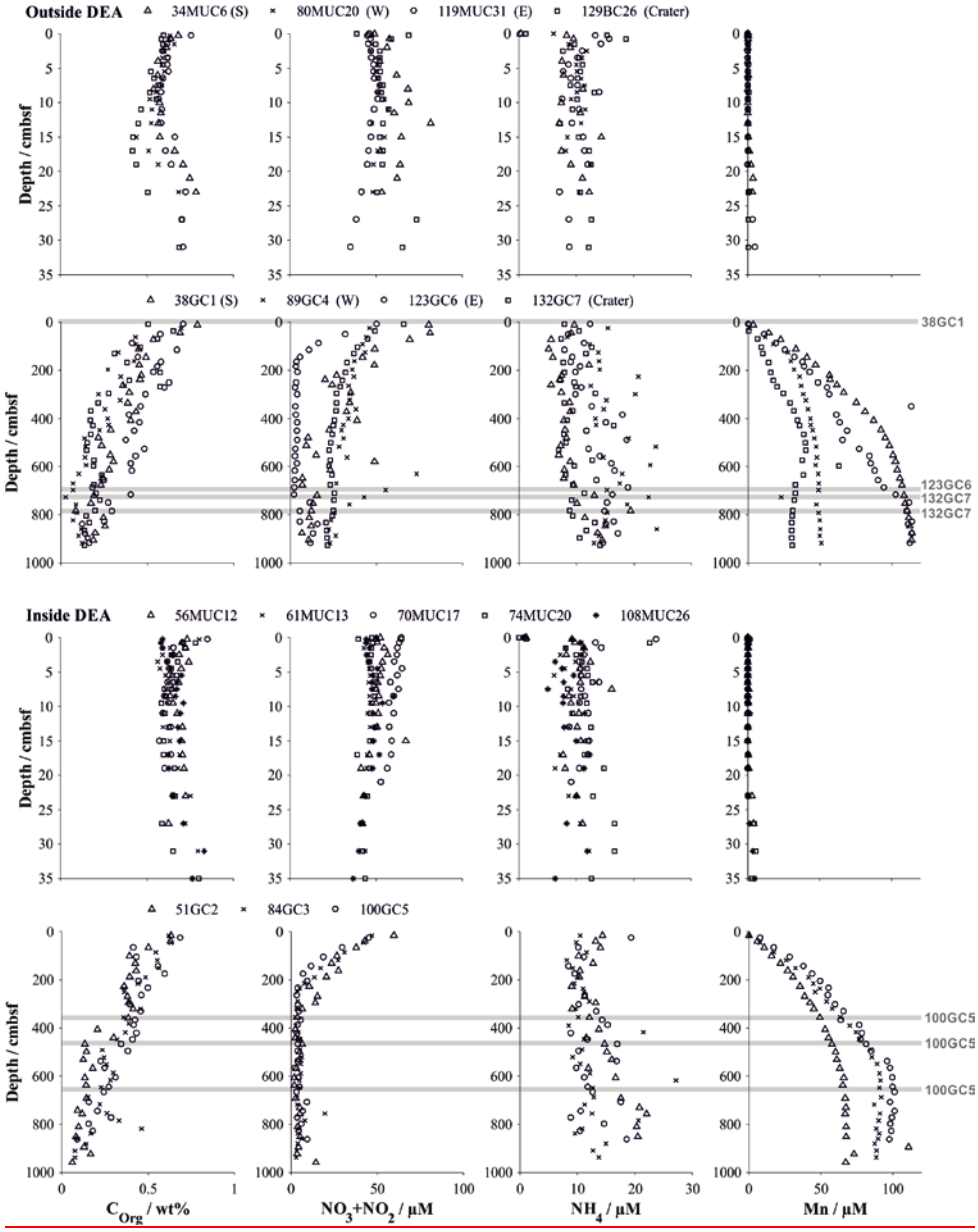
Outside DEA
34MUC6 (S)
80MUC20 (W)
119MUC31 (E)
129BC26 (Crater)
38GC1 (S)
89GC4 (W)
123GC6 (E)
132GC7 (Crater)
38GC1
123GC6
132GC7
132GC7
Inside DEA
56MUC12
61MUC13
70MUC17
74MUC20
108MUC26
51GC2
84GC3
100GC5
100GC5
100GC5
Depth / cmbsf
C_Org / wt%
NO3+NO2 / µM
NH4 / µM
Mn / µM

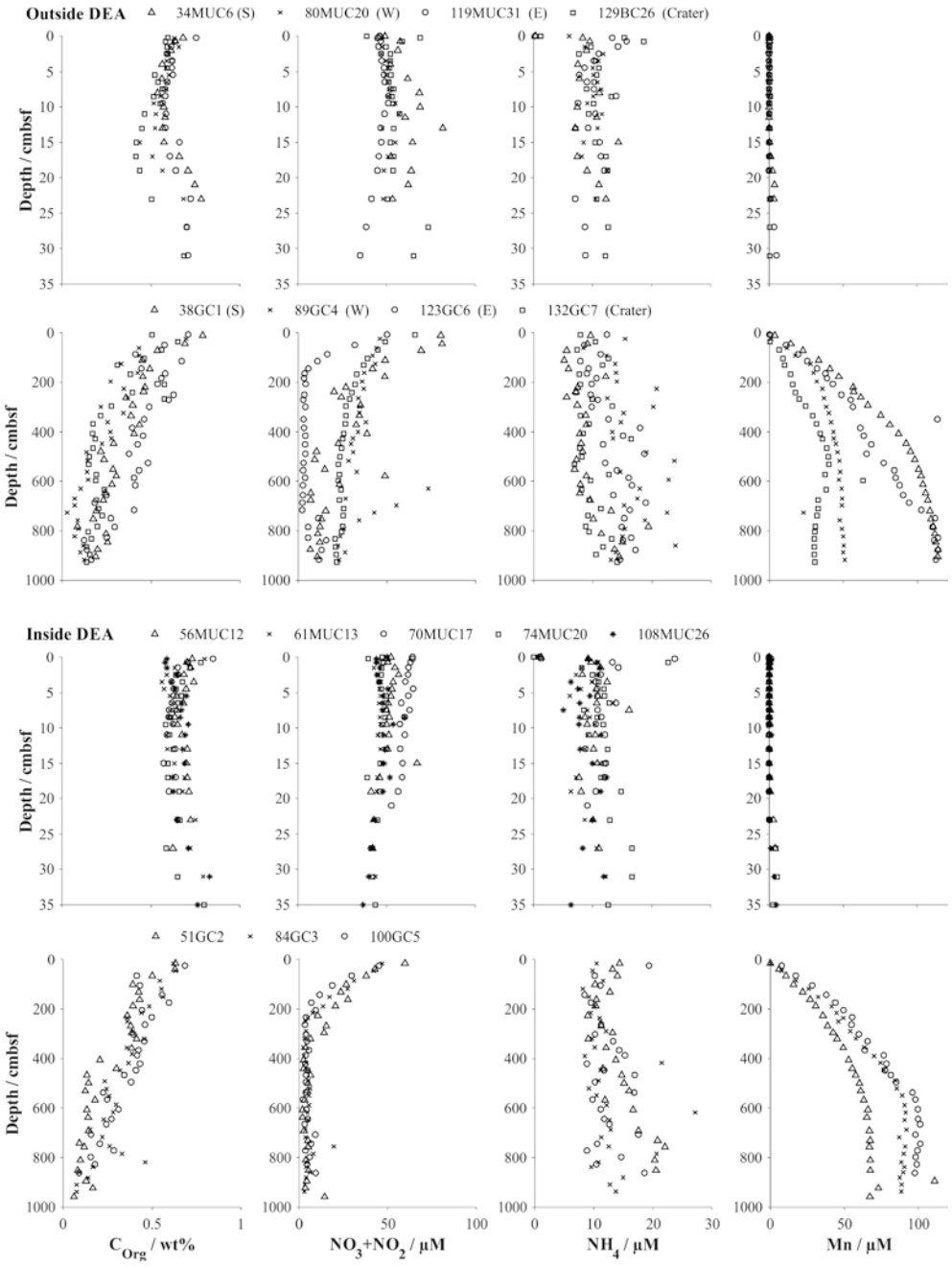

Figure 3. Organic carbon content (Paul et al., 2018; Paul et al., 2019) and ~~Informative solute~~dissolved solute profiles of summed NO_3 and NO_2 (Paul et al., 2018; Paul et al., 2019), NH_4 and Mn ~~, organic carbon content (Paul et al., 2019) and porosity~~ in gravity cores and their corresponding multicores~~(Paul et al., 2018)~~. Symbols represent the measured values at the mean depth of the sediment layer sampled. Buried manganese nodules are indicated by a grey line. Details on individual sampling stations can be found in Table 1.

Formatted: Subscript

Formatted: Subscript

Formatted: Subscript

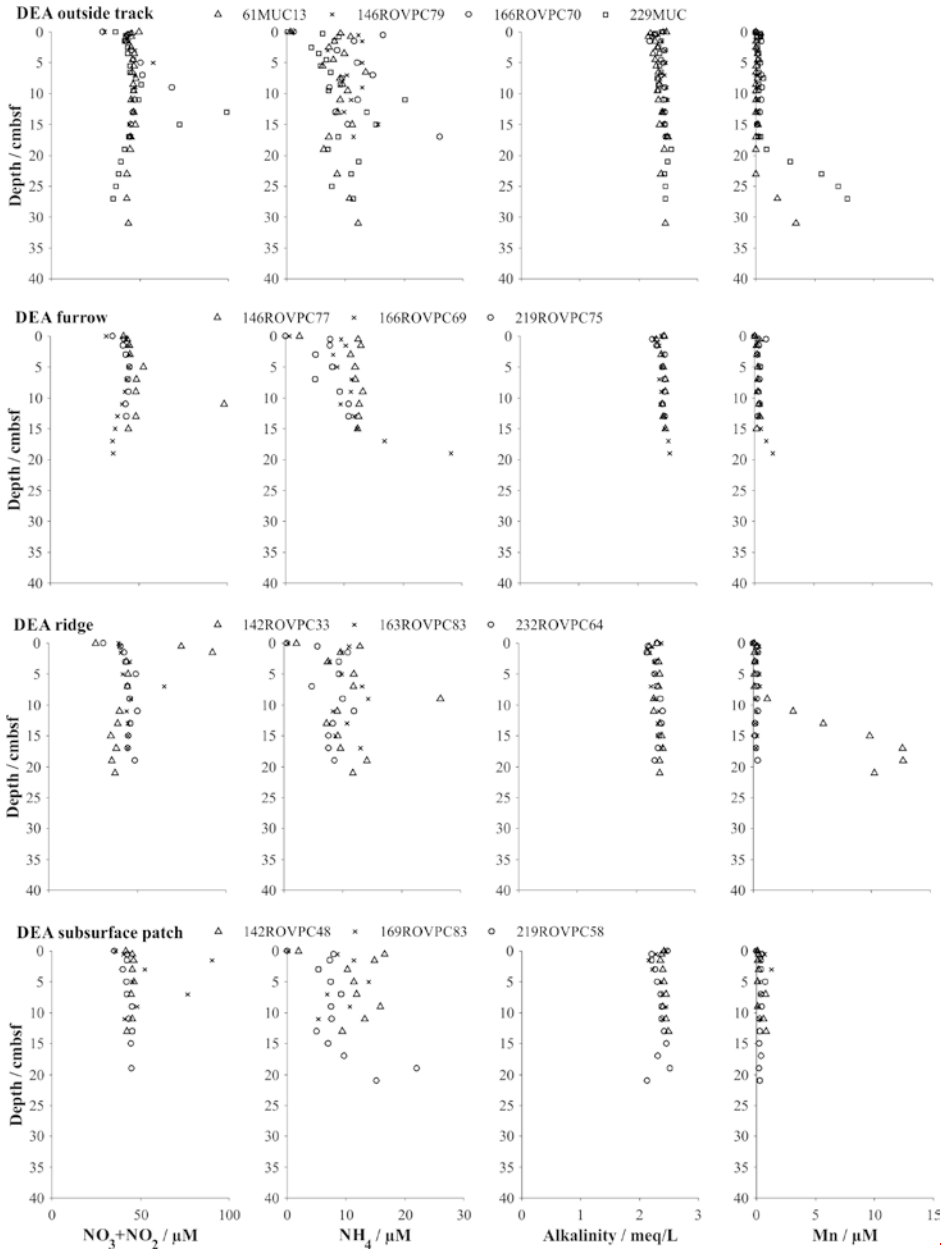

760 **Figure 4.** Solute profiles in multi- and box-corer retrieved in various microhabitats. Symbols represent the measured values at the mean depth of the sediment layer sampledPaul et al. (2018). Details on individual sampling stations can be found in Table 1.

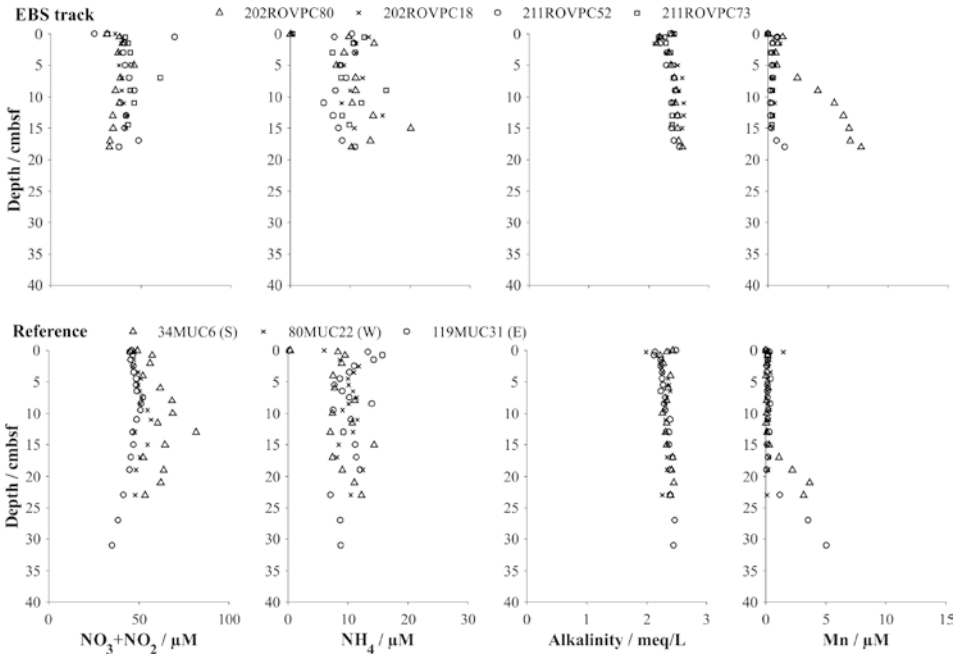

765 **~~Figure 4~~**. ~~Cont'd.~~

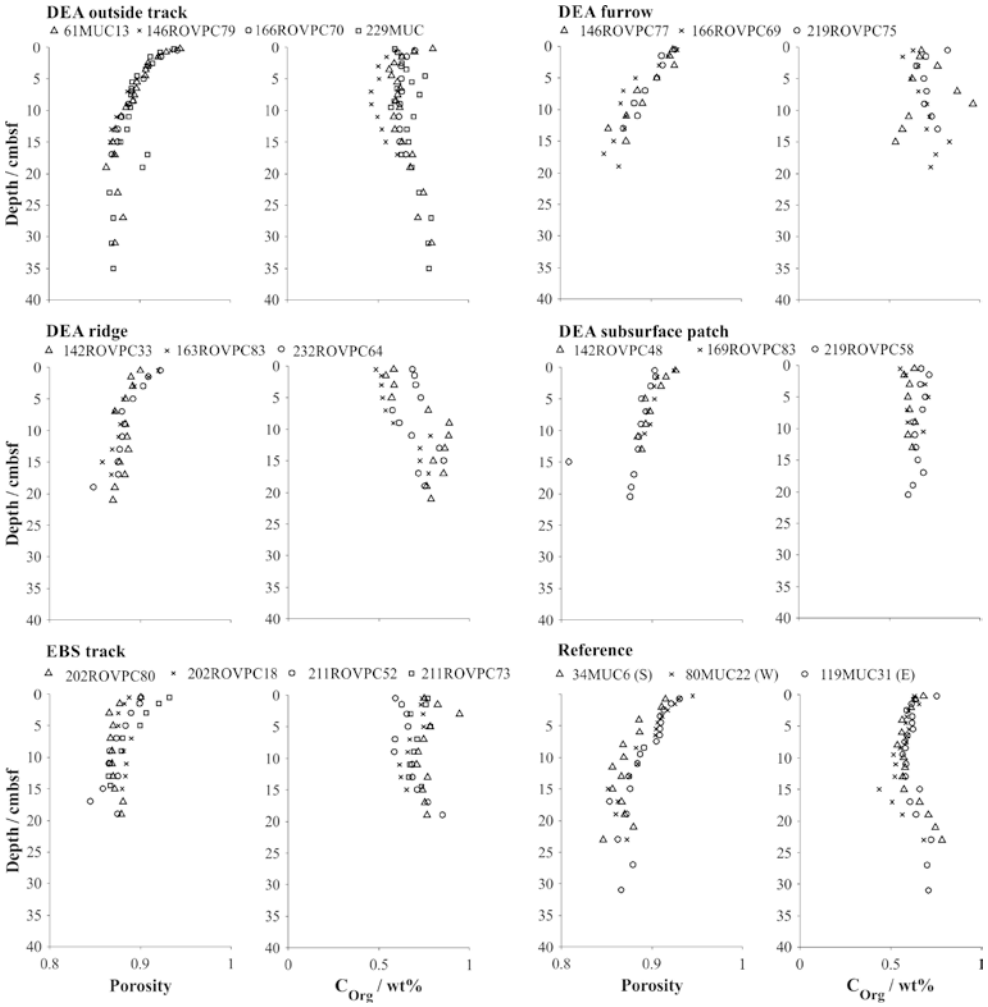

Figure ~~5~~4. Porosity and organic carbon content in multi- and box-corer retrieved in various microhabitats (Paul et al., 2018). Symbols represent the measured values at the mean depth of the sediment layer sampled. Details on individual sampling stations can be found in Table 1.

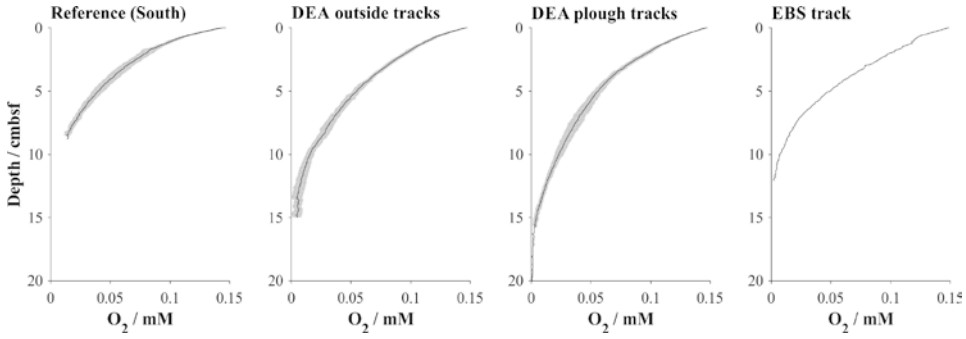

Figure ~~6~~5. Averaged (black line) in situ oxygen profile representative of various disturbance settings including their standard deviations (shaded area). Because the depth steps between each measuring point of the oxygen profiles are very close, they are not resolved in the diagram. Details on individual sampling stations can be found in Table 1.

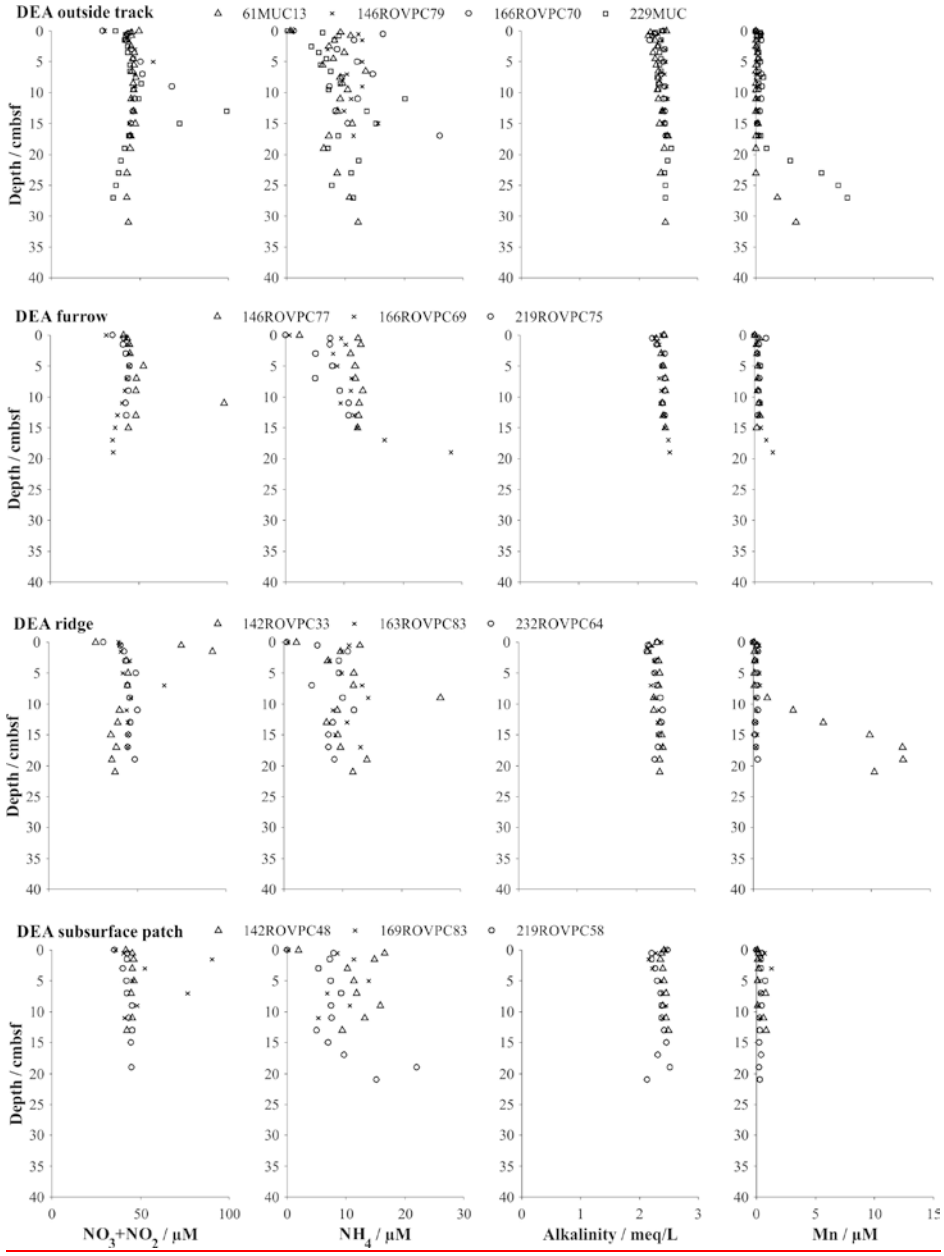

780

Figure 6. Solute profiles in multi- and box-corer retrieved in various microhabitats (. Symbols represent the measured values at the mean depth of the sediment layer sampled (summed NO_3 and NO_2 from Paul et al. (2018)). Details on individual sampling stations can be found in Table 1.

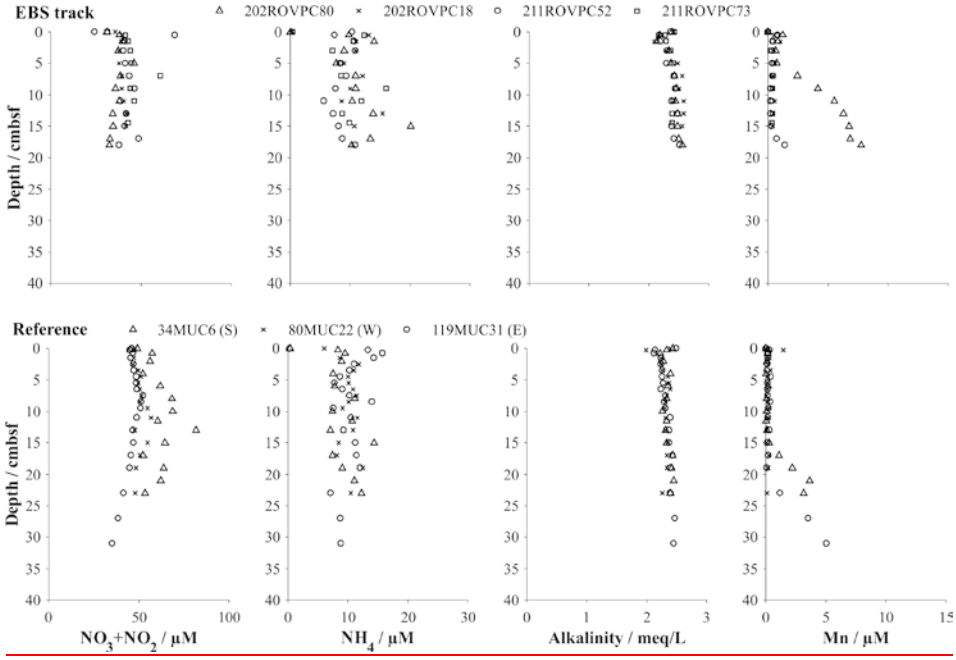

Figure 6. Cont'd.

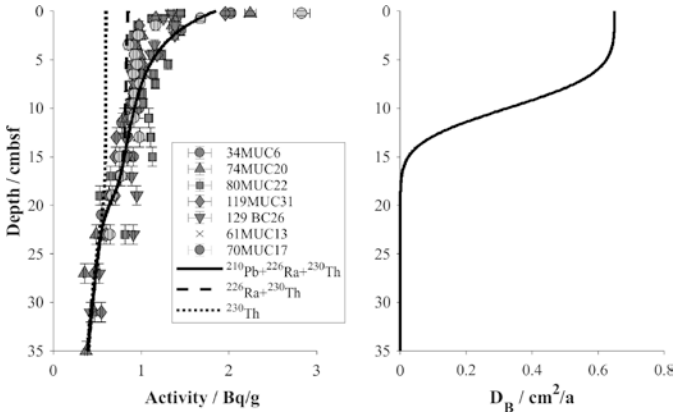

Figure 7. Model results of the faunal bioturbation activity in reference and DEA-outside track sediments based on measured ^{210}Pb activities. Left: Model curves indicate total ^{210}Pb activity (solid) and supported contributions by ^{230}Th (dotted) and ^{226}Ra (dashed minus dotted). Right: Bioturbation intensity profile derived for the background model.

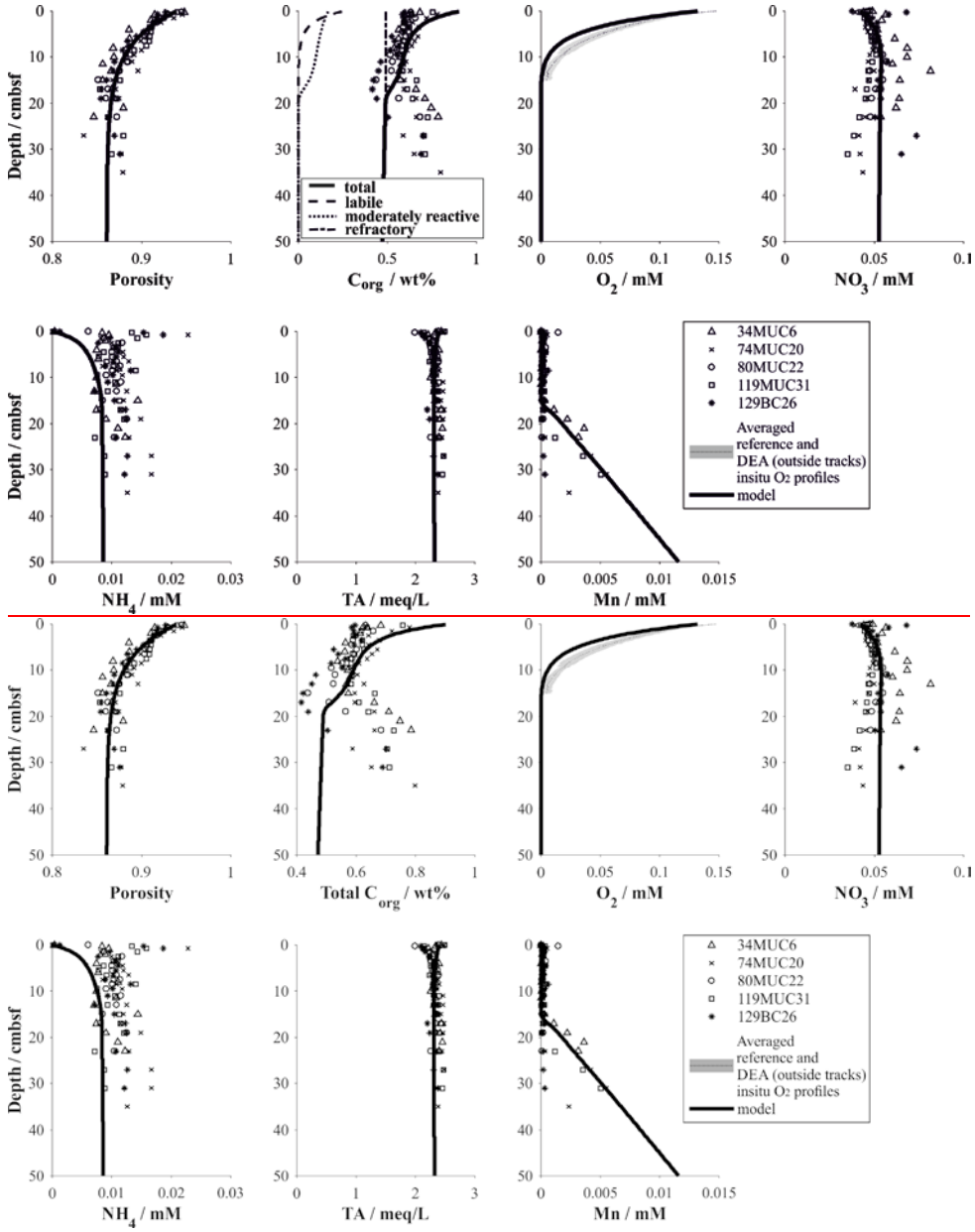

Figure 8. Simulation of background biogeochemical processes and their effect on solute profiles in the DEA region. In addition to the three reference stations, two other undisturbed sites were included for comparison. See Table 4 for parameterization of the modelled profiles.

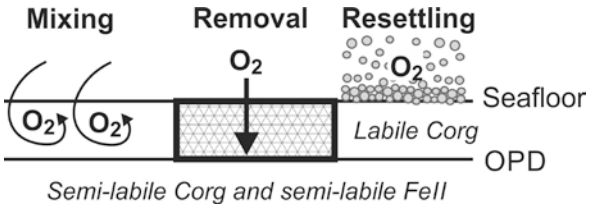

Figure 9. Schematic characterization of the different impact types at a mined seafloor and their influence on O_2 distribution.

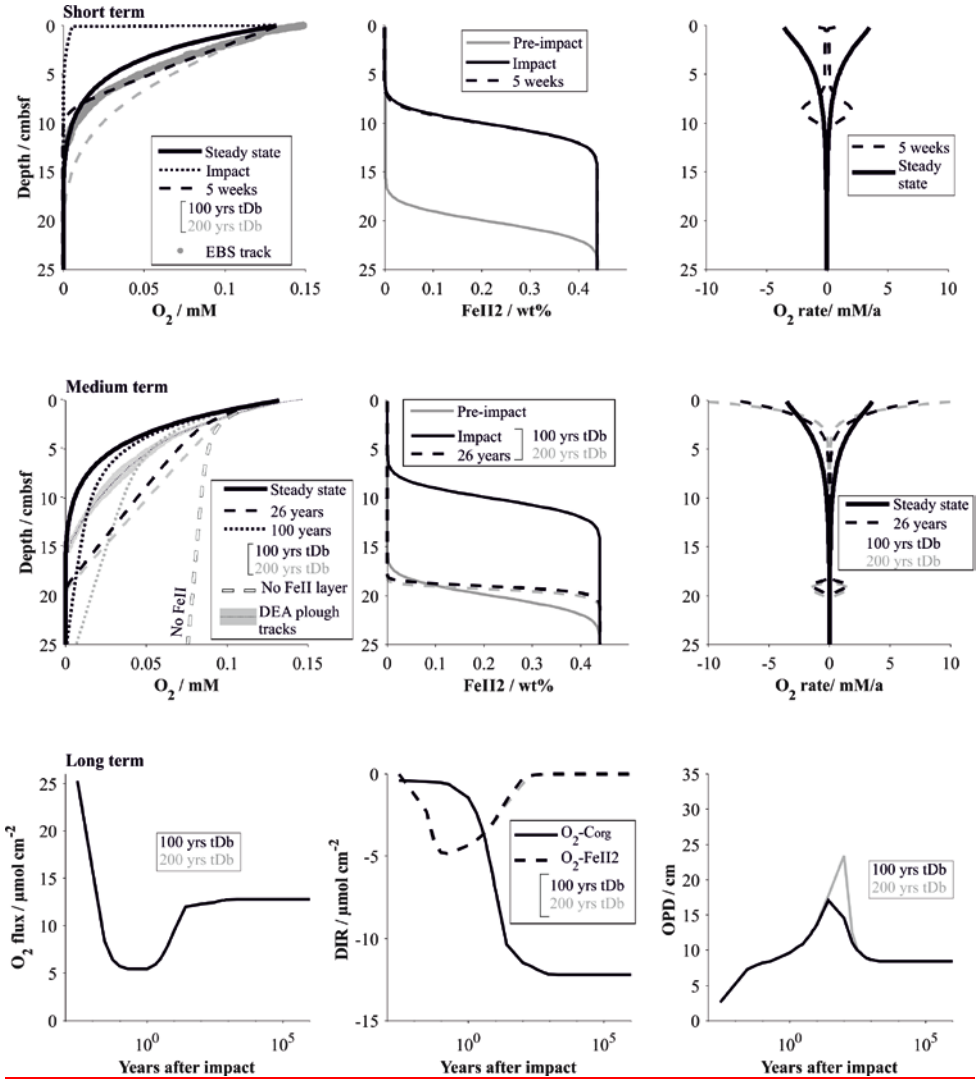
Short term
Depth / cmbsf
O2 / mM
Steady state
Impact
5 weeks
100 yrs tDb
200 yrs tDb
EBS track
Pre-impact
Impact
5 weeks
FeII2 / wt%
5 weeks
Steady state
O2 rate/ mM/a
Medium term
Depth / cmbsf
O2 / mM
Steady state
26 years
100 years
100 yrs tDb
200 yrs tDb
No FeII layer
DEA plough tracks
No FeII
Pre-impact
Impact
26 years
100 yrs tDb
200 yrs tDb
FeII2 / wt%
Steady state
26 years
100 yrs tDb
200 yrs tDb
O2 rate/ mM/a
Long term
O2 flux / µmol cm-2
100 yrs tDb
200 yrs tDb
Years after impact
DIR / µmol cm-2
O2-Corg
O2-FeII2
100 yrs tDb
200 yrs tDb
Years after impact
OPD / cm
100 yrs tDb
200 yrs tDb
Years after impact

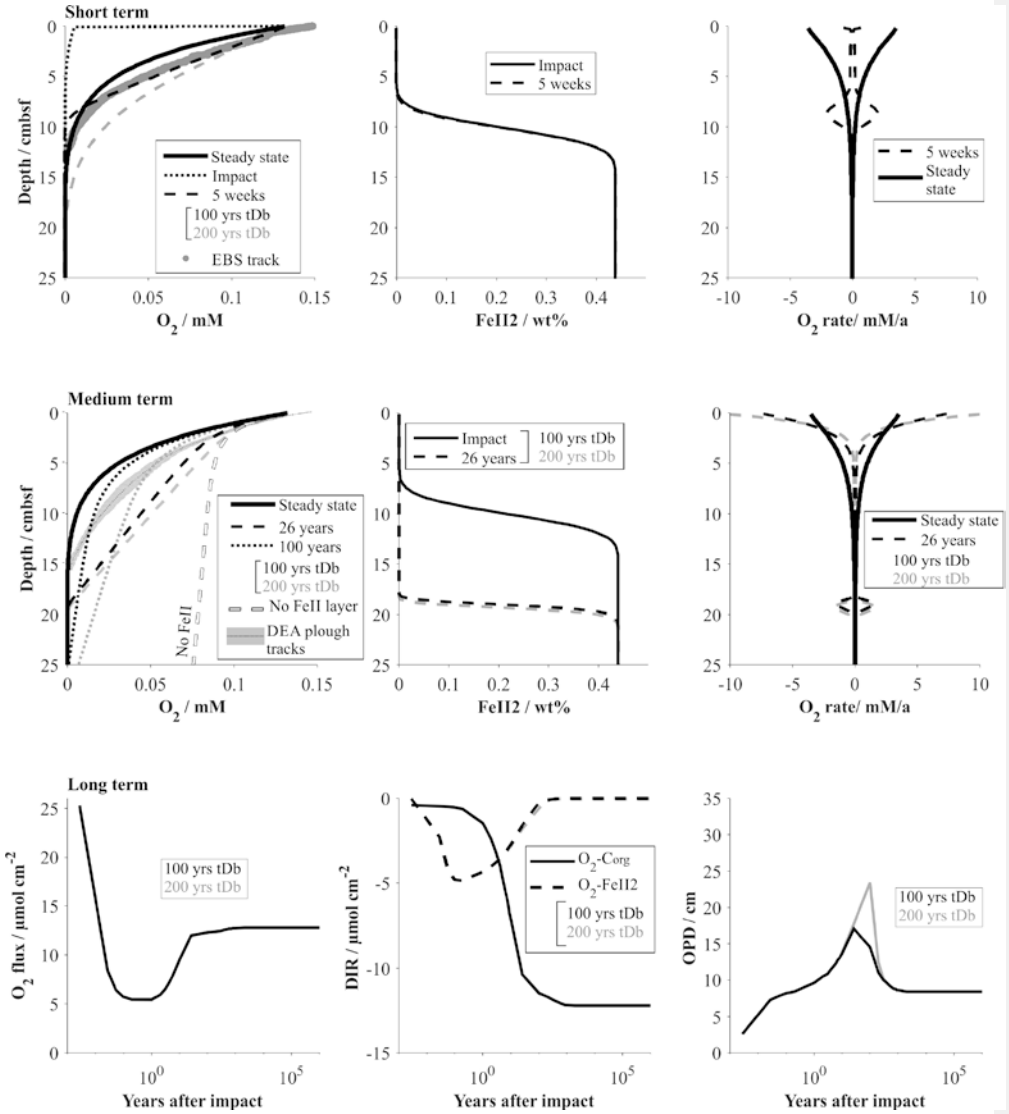

Figure 10. Impact simulations after a disturbance causing the reactive upper 10 cm to be removed. The short term (up to 5 weeks, comparable to the EBS tracks) and medium term (26 years, comparable to the DEA tracks) impact is visualized by the respective O_2 profiles and the fluxes shaping the O_2 profiles. It is assumed that the oxygen penetration depth is impeded by a reactive Fe(II) layer. Note, the Fe(II) is assumed to be located at 20 cmbsf but is placed at 10 cm if the upper 10 cm are removed. For comparison the O_2 profile in the absence of a Fe(II) layer is also shown. The long term impact is demonstrated by the surface flux of oxygen into the sediment, the depth integrated reaction rates (DIR) of oxygen with organic matter (C_{org}) and with the reactive Fe(II) layer, as well as the oxygen penetration depth (OPD) over time. The influence of the bioturbation recovery time is shown by plotting the lines that correspond to a recovery interval of 100 and 200 years in black and grey respectively.

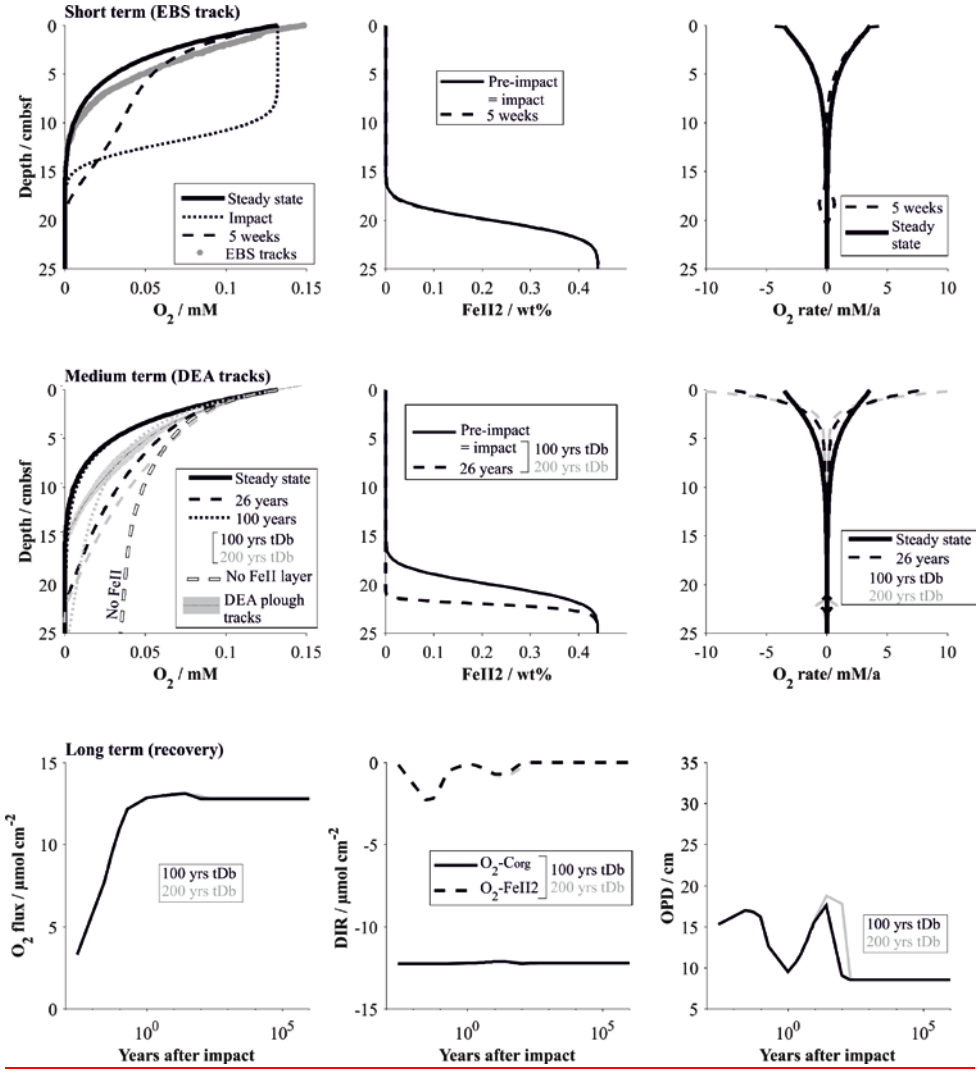
Short term (EBS track)
Depth / cmbsf
Steady state
Impact
5 weeks
EBS tracks
O2 / mM
Pre-impact
= impact
5 weeks
FeII2 / wt%
5 weeks
Steady state
O2 rate/ mM/a
Medium term (DEA tracks)
Depth / cmbsf
Steady state
26 years
100 years
100 yrs tDb
200 yrs tDb
No FeII layer
DEA plough tracks
No FeII
O2 / mM
Pre-impact
= impact
26 years
100 yrs tDb
200 yrs tDb
FeII2 / wt%
Steady state
26 years
100 yrs tDb
200 yrs tDb
O2 rate/ mM/a
Long term (recovery)
O2 flux / µmol cm-2
100 yrs tDb
200 yrs tDb
Years after impact
DIR / µmol cm-2
O2-Corg
O2-FeII2
100 yrs tDb
200 yrs tDb
Years after impact
OPD / cm
100 yrs tDb
200 yrs tDb
Years after impact

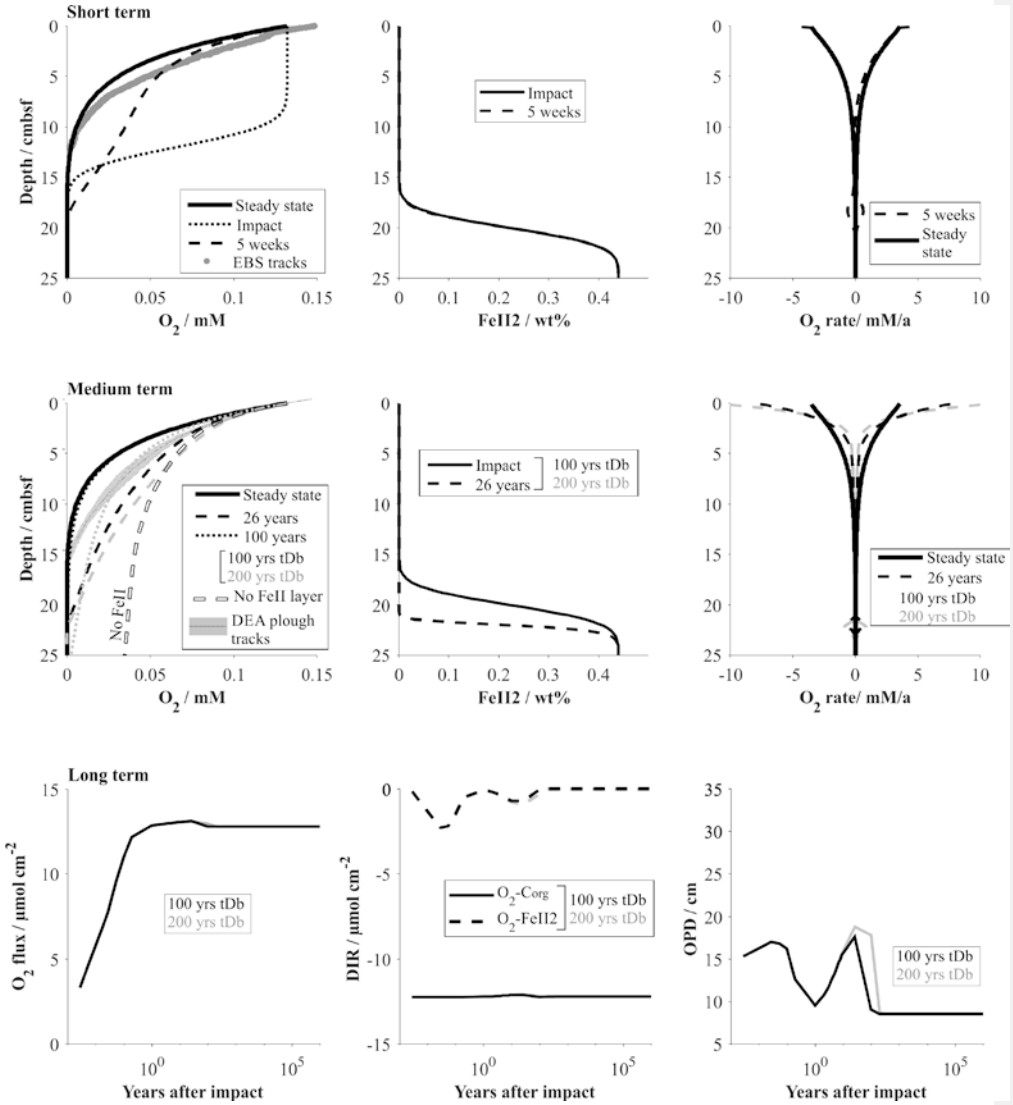

825 **Figure 11**. Impact simulations after a disturbance causing the upper sediment layer to be exposed to bottom water oxygen levels (i.e. through mixing or by resettling sediments, see Figure 9). See the caption of Figure 10 for details.

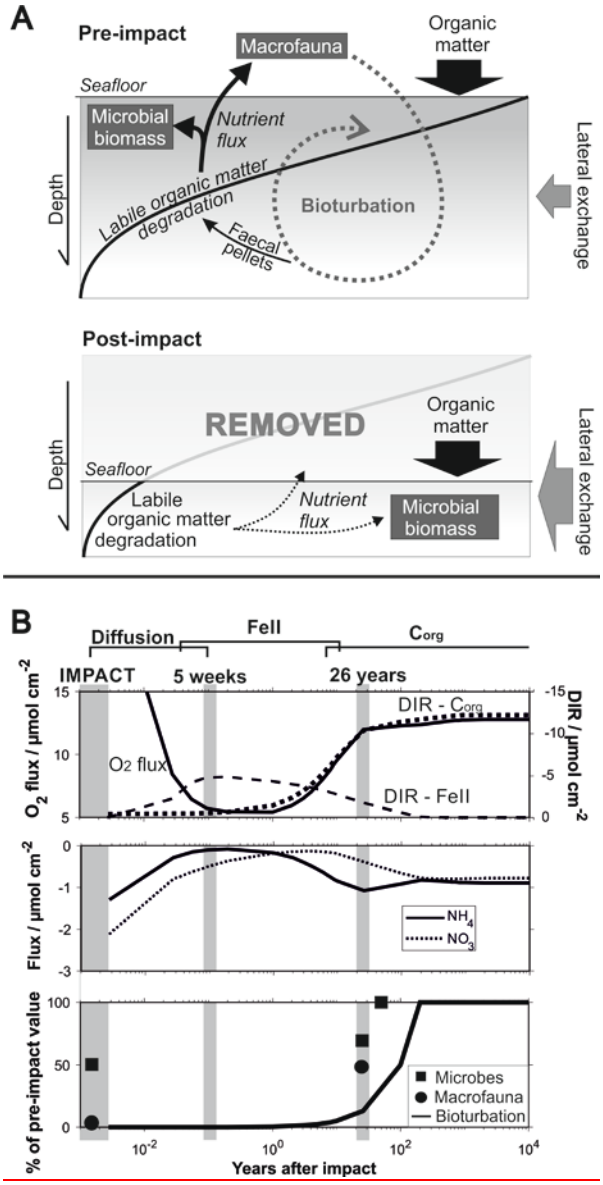
A
Pre-impact
Macrofauna
Organic matter
Seafloor
Microbial biomass
Nutrient flux
Depth
Labile organic matter degradation
Bioturbation
Faecal pellets
Lateral exchange
Post-impact
REMOVED
Organic matter
Depth
Seafloor
Labile organic matter degradation
Nutrient flux
Microbial biomass
Lateral exchange
B
Diffusion
FeII
Corg
IMPACT
5 weeks
26 years
O2 flux / µmol cm-2
DIR - Corg
O2 flux
DIR - FeII
DIR / µmol cm-2
Flux / µmol cm-2
NH4
NO3
% of pre-impact value
Microbes
Macrofauna
Bioturbation
Years after impact

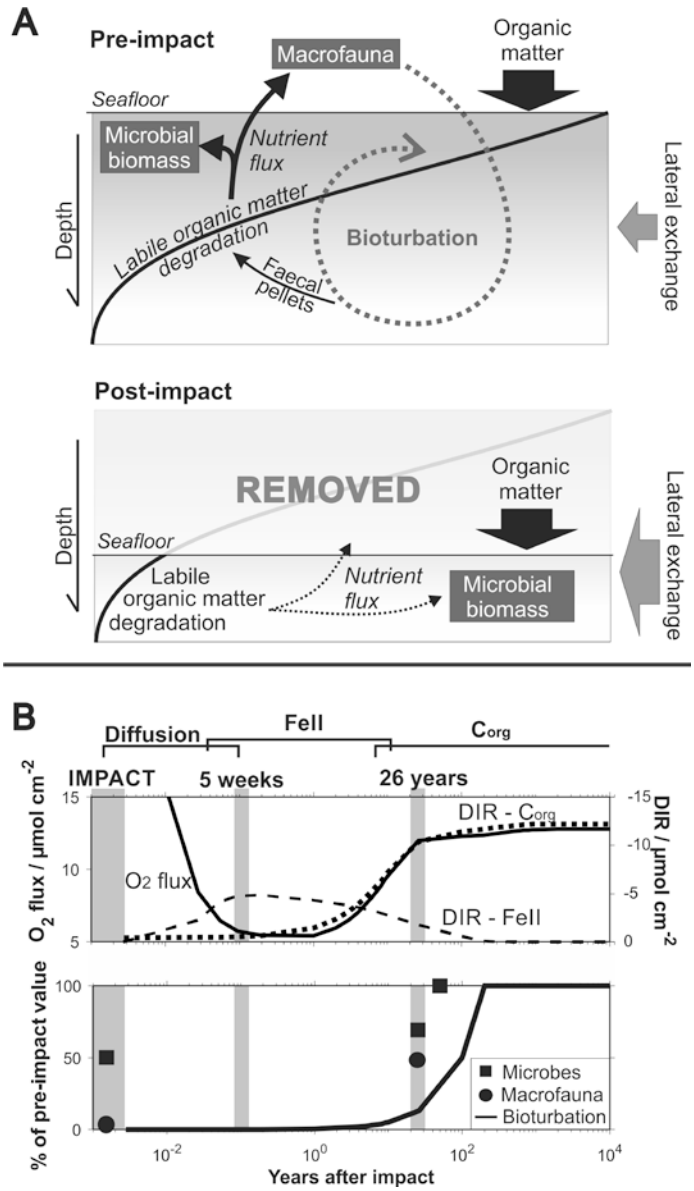

Figure 12. (A) Schematic diagram showing the delicate interplay between the distribution of organic matter, microbial activity and the bioturbation through burrowing megafauna in a pre-impact system and after removal of the upper reactive sediment layer. (B) Quantitative comparison of geochemical and biological processes over time after an impact through sediment removal. Biological data is taken from Stratmann et al. (2018a) (Macrofaunal abundance) and Vonnahme et al. (in press) (microbial cell cout) for the most severely disturbed sites (e.g. inside 5 weeks old EBS tracks, and inside 26 years old plough marks).